Lawrence Berkeley Laboratory
UNIVERSITY OF CALIFORNIA
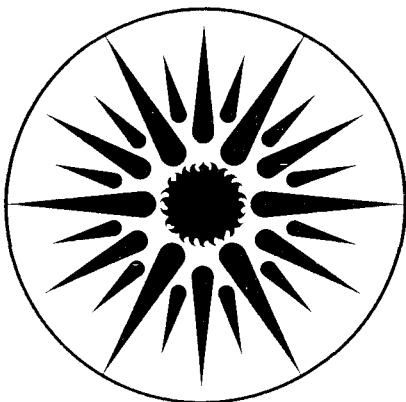
APPLIED SCIENCE DIVISION

**Monitoring and Modeling for Radon Entry
into Basements: A Status Report for
the Small Structures Project**

W.J. Fisk, S. Flexser, A.J. Gadgil, H.-Y. Holman,
M.P. Modera, T.N. Narasimhan, T. Nuzum, K.L. Revzan,
R.G. Sextro, A.R. Smith, Y.W. Tsang, and H.A. Wollenberg

September 1989

**APPLIED SCIENCE
DIVISION**

MONITORING AND MODELING OF RADON ENTRY INTO BASEMENTS:

A STATUS REPORT FOR THE SMALL STRUCTURES PROJECT

W.J. Fisk, S. Flexser, A.J. Gadgil, H.-Y. Holman, M.P. Modera, T.N. Narasimhan, T. Nuzum,

K.L. Revzan, R.G. Sextro, A.R. Smith, Y.W. Tsang and H.A. Wollenberg

September 1989

Indoor Environment Program

Applied Science Division

and

Earth Sciences Division

Lawrence Berkeley Laboratory

1 Cyclotron Road

Berkeley, California 94720

ABSTRACT

The approach, status, and initial findings of a research project on radon transport through soil and entry into buildings are described. For the experimental component of this project, we have constructed two room-size precisely-fabricated basements at a site with relatively homogeneous soil. The structures, which are distinct only due to the presence (or absence) of a layer of aggregate beneath the floor, have adjustable-size openings to the soil, are otherwise very air-tight, and are mechanically ventilated using a system that also controls the indoor-outdoor pressure difference. Numerous probes have been installed in the soil surrounding the structures to permit multipoint measurement of soil moisture content, soil temperature, permeability of soil to air, soil-gas pressure, and radon concentration. State-of-the-art instrumentation is being installed for real-time monitoring of these parameters plus structure ventilation rate, indoor and entering soil-gas radon concentrations, and meteorologic parameters for a period of at least one year. Many of the factors that control or influence radon entry will be modified intentionally or by changes in environmental parameters during the course of the measurements. To develop a suitable instrumentation system, we have found it necessary to design and fabricate a new type of probe for more accurate measurements of soil permeability. We have also verified and improved procedures for more accurate, rapid, multipoint measurements of radon concentrations using a continuous radon monitor. Identical structures, with the same instrumentation, will be constructed at additional sites with different soil characteristics and climates. Core samples of the soil from each site are analyzed to determine density, porosity, permeability, radium content, and radon emmanation coefficient. The research project also includes steady-state and transient numerical modeling efforts that complement the experimental research and that will use the experimental data for model validation. Steady-state modeling has indicated that buoyancy effects on soil-gas flow (due to heat loss from the substructure) and layers of subslab aggregate can cause large increases in radon entry rates. The effects of a variety of structural and soil properties, including heterogeneous features of the soil, are also being investigated with a steady-state model. In addition, the model has been used to determine that the very broad range in soil permeabilities is consistent with the narrower distribution in indoor radon concentrations. The transient numerical modeling is focusing on an evaluation of the importance of transient soil-gas flow primarily in response to temporal variations in atmospheric pressure. Preliminary results indicate that transient flow may be very important in low-permeability soils where radon entry due to steady-state flow is limited. The modeling efforts, combined with the experimental findings, should substantially advance our understanding of the mechanisms of radon entry and the dependence of radon entry rates on soil, structural, and climactic factors.

INTRODUCTION AND OVERALL PROJECT DESCRIPTION

The sources of indoor radon (^{222}Rn) are the soil surrounding the building's substructure, outdoor air, earth-based building materials, and water (predominantly water from local private wells) (Nazaroff and Nero 1988). The surrounding soil is usually the dominant radon source in buildings with even moderately elevated radon concentrations. Radon is produced within the soil by the radioactive decay of radium, which is present in all crustal materials, and is transported within the soil both by molecular diffusion and the advective (pressure-driven) flow of soil gas.

Pressure-driven flow of soil gas into structures, through penetrations (cracks, joints, and holes) that extend between indoors and the soil, is considered to be the dominant process of radon entry into most buildings. The small ($\leq$ 10 Pa) pressure differences that drive this entry result primarily from: the reduced density of heated indoor air relative to the density of outdoor air, wind, and mechanical systems within the building, such as exhaust fans, that cause a net flow of air to outdoors. Decreases in barometric pressure, which may be larger in magnitude, can also drive soil-gas flow into buildings.

The process of radon entry into houses with basements has been investigated experimentally, in part, by long-term (e.g., full-year) monitoring of numerous parameters in occupied houses (see, for example: Nazaroff et al. 1985; Turk et al. 1989; Revzan 1989; Turk et al. 1988). Parameters monitored include pressures, temperatures, and radon concentrations indoors and in the soil, soil permeability, furnace operation, and outdoor environmental conditions. These field studies also included analyses of the radium content of soil samples and measurements of the radon exhalation rate from building materials and the concentrations of radon in the domestic water supply. Although much valuable information has been obtained through these studies, they have not provided data of sufficient quality and detail to fully develop or validate theories and models of radon entry. For example, the nature and location of penetrations to the soil and the permeability of backfill and aggregate adjacent to the exterior surfaces of basements are two of the many parameters that are not readily characterized (or controlled by the experimenters) at the site of actual houses.

Radon entry processes have also been investigated through the development and use of models (primarily numerical models) of soil gas and radon transport (e.g., Loureiro 1987; Mowris and Fisk 1988; Revzan 1989; Revzan et al. 1989). However, previous models have not accounted for many potentially important factors such as transient flow, buoyancy-driven flow, and highly heterogeneous soils.

This report describes the approach, status, and initial findings of an interdisciplinary research effort entitled "Experimental and Theoretical Investigation of Radon Availability, Migration, and Entry," commonly called the "Small Structures" project, with the goal of substantially advancing and confirming our understanding of radon entry into basements through experimentation and mathematical modeling. Specific objectives include quantifying the effects of different transport mechanisms, driving forces, and controlling parameters on the radon entry process, including: (1)

soil characteristics including soil permeability, radium content, soil moisture, freezing at the soil surface, and heterogeneous features of the soil; (2) building characteristics including the size and location of penetrations to the soil and the presence of subslab aggregate; (3) steady-state and time-varying indoor-outdoor pressure differences caused by a variety of factors; and (4) meteorological factors such as temperature, wind, precipitation, and barometric pressure changes. Project objectives also include the development and validation of advanced models of radon entry. The experimental and modeling efforts are closely linked. Models have been used to guide the design of the structure and instrumentation system and to help guide the selection of experimental procedures. The experimental data will be the source for model validation.

In the experimental component of this project, we have constructed two precisely designed and fabricated room-size basements at the first of several sites. The experimental sites are selected based on our experimental objectives and characterized in detail. Most of the characterization of the first site has been completed. An instrumentation system is presently being installed for monitoring of several soil and soil-gas properties (at multiple locations) and indoor and outdoor conditions (including radon concentrations) over a period of one year or more. At each site, we will study the influence of structural factors, steady-state and time-varying driving forces, and naturally varying soil and climatic properties on the radon entry rate. The dependence of radon availability and entry on geologic and climatic factors that vary between sites will be determined by comparing the results of measurements at different sites in light of the insights gained from the modeling effort. The experimental effort has required that we improve upon previously used instrumentation, probes, and data analysis techniques. The instrumentation, structures, and experimental procedures are designed to test theories about radon entry processes (e.g., the hypothesis that atmospheric pressure changes can cause a pumping of soil gas into and out of substructures) and so that the intermediate results of models (e.g., soil gas pressures) and final results (e.g., radon entry rates) can be checked. A key part of this effort has been the refinement, verification, and application of steady-state and transient numerical models of radon transport into buildings. In addition to providing guidance to the experimental work, the models have been (and are being) used to advance our understanding of the radon entry process and the influence of various factors on the radon entry rate.

This report describes the approach, progress, and accomplishments to date of the Small Structures Project. The experimental and theoretical elements of the research are described in separate sections on: (1) site selection and characterization, (2) structure design and construction, (3) instrumentation, (4) experimental plans, (5) modeling objectives, (6) steady-state modeling, and (7) transient modeling.

SELECTION AND CHARACTERIZATION OF THE SMALL STRUCTURES SITE

This section discusses the considerations and activities that led to the choice of the first experimental site at Ben Lomond Mountain, California, the characteristics of that site, and considerations for selection of a second site. The essence of this first experimental set-up, which is described in detail in the next section, is that two nearly identical small structures (basements) were built with one principal difference: one structure's floor slab rests directly on the soil, the other's slab rests on aggregate (gravel). The structures, nominally 2.3 by 3.5 m (7.7 by 11.5 ft.) in plan (including the thickness of the walls) and 2.3 m (7.5 ft.) high, were emplaced in excavations 2.1 m (7 ft.) deep and surrounded on their sides by a ~0.75 m (2.5 ft.) wide zone of compacted backfill.

Criteria for Selecting the Initial Site

Desired characteristics of the initial site include soil conditions that are as uniform as possible over the volume that encompasses both structures, and soil that is relatively homogeneous on a scale of a few centimeters. An idealized setting was considered to be one with a deep soil with no significant lithologic or structural discontinuities within at least 3 to 4 m (10 to 12 ft.) in any direction from the structures. Therefore, sites were sought on deep, uniform alluvial soil, or on residual soil developed from deep weathering of rock. Since the effect of soil moisture on the entry rate ingress of radon into a structure is an important consideration, a site with strongly contrasting rainy and dry seasons was desirable. This would permit measurements to be made under differing degrees of partial soil saturation. It was also desirable that the permanent water table be at least one excavation depth (~2 m) below the bottom of the structure. A soil with an appreciable, but not necessarily high permeability and radium concentration, and good radon emanation was also

necessary. It was considered that the initial site should be within reasonable driving distance from Lawrence Berkeley Laboratory (LBL) and should have good access to electrical power lines and telephone communications.

Screening and Characterization

To select the initial site, geological settings and soil characteristics of coastal central California were assessed in regard to the above criteria. Geological reports and maps of the California Division of Mines and Geology and the U.S. Geological Survey were consulted, as were county soils reports of the U.S. Soil Conservation Service. Interpretation of the geologic reports identified areas of appreciable radon concentration based on the presence of rocks with known moderate to high uranium concentration (Wollenberg and Revzan, 1989). The soils reports were valuable in focusing on sites in areas where climates appeared favorable and soils were well developed and of moderate to high permeability. (The permeabilities expressed in Soil Conservation Reports are for liquids, based on the rate of infiltration of a column of water into the soil, and can be correlated with the air permeability of soil as discussed by Nazaroff et al. (1989a)).

Six potential sites were examined in the San Francisco Bay Area (Figure 1); their characteristics are listed in Table 1. Radium concentrations were determined initially by field measurements of the gamma radioactivity around the 1.76 MeV photopeak of bismuth-214, a member of the uranium decay series. These measurements were followed, and in large part confirmed, by laboratory gamma spectrometry of samples collected from the surfaces of the sites. The radon emanation fraction (the ratio of radon emanated to radon produced) of these samples was also measured in the laboratory. At three of the sites, i.e., Ben Lomond, Las Posadas, and Oxford Tract, soil auger samples were collected at 15 cm (6 in.) intervals over a total depth of 1.5 m (5 ft.), and were analyzed in the laboratory for their radium concentrations and radon emanation rates. These three sites were also studied, using temporarily installed probes, to determine, in situ, their permeabilities and radon concentrations, using methods described by Garbesi (1988). Modifications of these methods will be used for repeated measurements of soil permeability and radon in soil gas at the small-structure sites, while soil moisture will be measured by time-domain reflectometry, as described in a subsequent section that discusses instrumentation.

6

At Oxford Tract and Las Posadas, permeabilities were relatively low compared to Ben Lomond, and given our field methods, these low permeabilities prohibited accurate field measurements of soil-gas radon concentrations. On the basis of results from Oxford Tract, a site within 1 km (0.6 miles) of LBL, the two other potential alluvial sites, Napa State Hospital and Camp Parks, were not examined further, nor was the Ink Grade site which has characteristics similar to those of Las Posadas. Because of the Ben Lomand's site's high seasonal rainfall, relatively homogeneous soil, moderate radium concentration with relatively high radon emanation, appreciable permeability, and accommodating infrastructure (access to electricity and telephone, and the hospitable attitude of personnel of the California Division of Forestry), the site at Ben Lomond State Nursery was selected for the initial small structures installation.

Characteristics of the Ben Lomond Site

The site is located at an altitude of 790 m (2600 ft.) on a broad-topped oak- and Douglas fir-studded ridge, Ben Lomond Mountain, ~12 km (7 miles) inland from the Pacific coast. Rainfall is high, due to the orographic effect of the ridge, and is generally confined to the period October - April. The principal characteristics of the Ben Lomond Site are listed in Table 2. The soil is a residual sandy loam, developed from weathered quartz diorite, which is encountered at depths of 1.5 to 2 m (4 to 6 ft.) (Leo, 1967; Bowman and Estrada, 1980). The most prominent activity following selection and prior to construction was to obtain core samples to augment permeability and radon data obtained from measurements made during the site selection process. The array of probes and core holes in relationship to the approximate location of the structures is shown in Figure 2, and the spatial distributions of soil-gas radon concentrations and permeability are shown in Figure 3. The cores were obtained primarily by pushing consecutive 7.6-cm (3-in.) diameter by 76-cm (30-in.) long Shelby tubes into the soil, using a Failing -750 drilling rig. Three of the holes reached depths of 3.6 m (12 ft.), one hole 4.3 m (14 ft.), and one 6.5 m (21.25 ft). In this deepest hole the bottom 3.4 m (11.25 ft.) was rotary cored and samples recovered in a Pitcher core barrel. In all holes the depth reached was at least twice the 1.8 m (6 ft.) depth of installation of the small structures. Permeabilities of cores from the depth interval 1.5 to 2.3 m (5 to 7.5 ft.) in each of the 5 holes were determined in the laboratory, and as shown in Table 2, their arithmetic mean values and standard deviations agree, reasonably, with those determined in-situ by probes from

the surface. Laboratory testing by a consultant of 2 cores from depths of 0.76 to 1.5 m (2.5 to 5 ft.), indicates dry soil densities ranging from 1.2 to $1.9g/cm^3$ (76 to 119 pounds/ft.^{3}), and moisture contents (i.e., mass of moisture divided by mass of dry soil) ranging from 10.4 to 19.7%. As well as indicating soil properties, these data were valuable in designing the structures' excavations and the subsequent backfilling operations.

The backfill zone surrounding the sides of the structures ranges in width from 0.7 to 0.9 m. Our goal was to achieve as homogeneous a backfill as possible. Soil from the excavations was blended, then emplaced in ~30 cm layers and compacted. Compaction was monitored and controlled by use of gamma-ray and neutron measurements of density and moisture content, respectively. Based on 26 field measurements, the dry density of the backfill averages 1.41($\pm$ 0.05) g/cm^3 [$\pm$ one standard deviation], the moisture content 17($\pm$ 2.2)%, and the relative compaction of the backfill (with respect to the maximum dry density) 84($\pm$ 3)%. Thus, good homogeneity within the backfill was attained.

The distribution with depth of radium and radon-emanating fraction in the soil, based on auger samples at 15 cm (6 in.) intervals, is shown in Figure 4. The relatively high radium zone between 80 and 110 cm depth is associated with the presence of scattered rock fragments with abundant feldspar. Preliminary fission-track radiography of soil-auger and nearby rock-outcrop samples shows that uranium in unweathered outcrops is associated with accessory minerals. In weathered outcrops and soil, however, uranium is mainly associated with strongly altered mineral grains and with iron-oxide-rich coatings on grain surfaces (in concentrations of several tens of ppm U, in contrast to 1 to 3 ppm (by weight) in the bulk soil). These coatings are most likely the primary loci of radon emanation in the soil.

Criteria for Next Site

The small structures at Ben Lomond are encompassed by relatively homogeneous residual soil, are situated well above the permanent water table but at a location where seasonal rainfall temporarily saturates the soil. It was desired that conditions at this initial site be relatively uniform spatially, (to minimize complexity) in some contrast to conditions at most housing sites, but similar, in some respects, to the highly uniform soil in the Spokane River Valley -- Rathdrum Prairie area where homes with elevated indoor radon concentrations have been studied. In this regard, the next

small-structures site will be more heterogeneous. One consideration is a site that more closely simulates the conditions at housing sites in high-radon areas of the eastern U.S. in the following ways:

- excavation in soil with quite variable permeability; a residual soil but probably with mixed soil and rock fragments,

- appreciable precipitation (75 - 102 cm (30 - 40 in.)/year) but more evenly distributed over time, so that there is less seasonal contrast in soil moisture, and the depth to the saturated zone is relatively shallow, and

- a climate with prolonged cold periods when the near-surface soil is frozen.

We have identified and completed initial site-characterization measurements at one potential New Jersey site with these general characteristics.

Another consideration is a site with sharply contrasting zones of permeability; for example, a small structure encompassed in a horizontally stratified setting of sandy and clayey beds. An alternative is a structure spanning a near-vertical discontinuity, such as a high-angle contact separating rock (and its associated residual soil) of contrasting permeability.

Because future sites will be relatively heterogeneous compared to the initial site, they will be more difficult to characterize. However, because they will be more typical of housing sites in most areas of present concern, results of the measurements in small structures there (and the associated modeling) will be very germane to the understanding of the mechanisms of radon entry under more complex soil conditions.
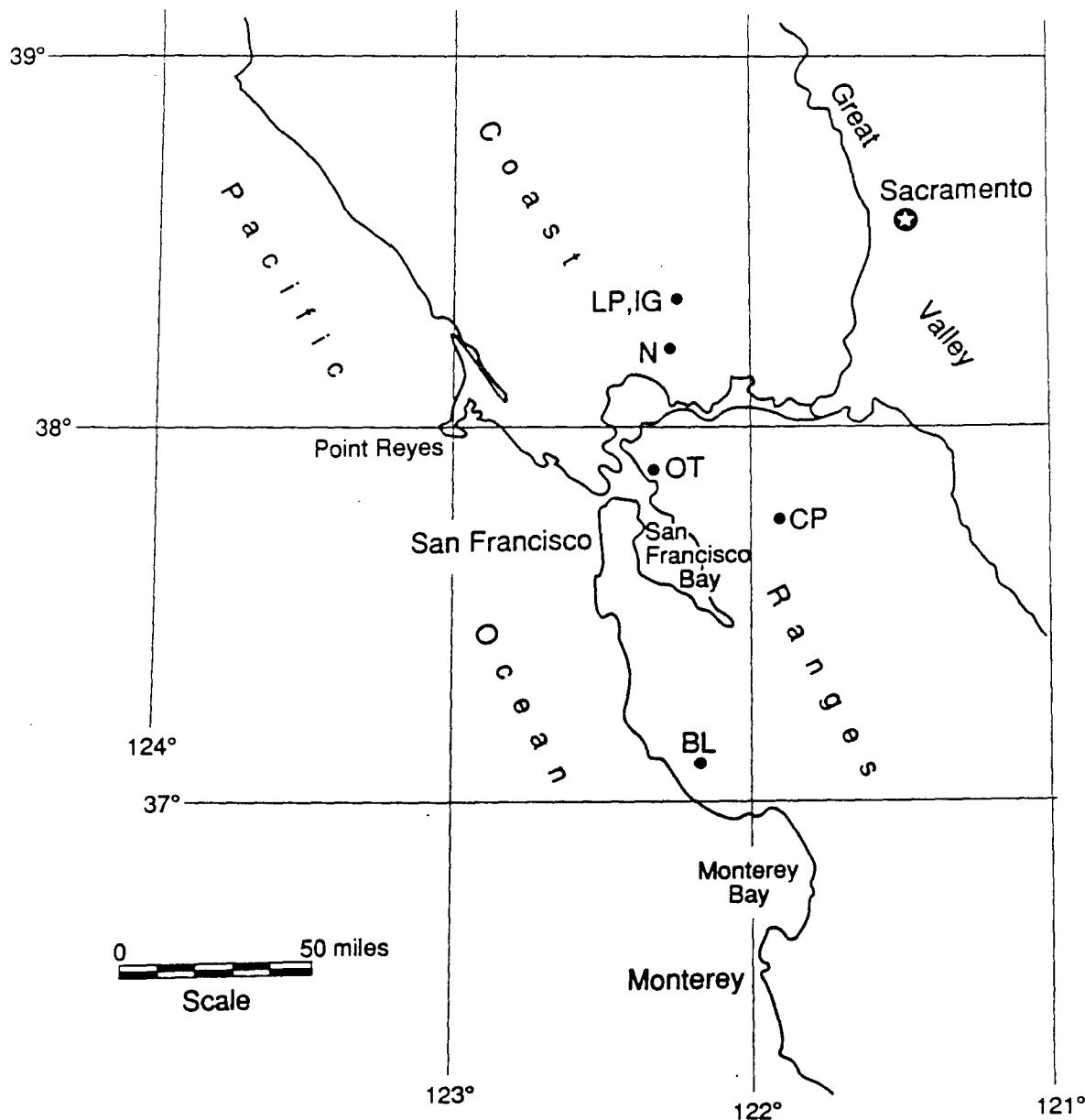
Table 1. Possible Initial Installation Sites

LOCATION	AVG. RAINFALL cm (in.)[a]	SOIL[a]	APPARENT ^{226}Ra Bq/kg [pCi/g]	SOIL-GAS ^{222}Rn Bq/m^3 [pCi/l]	EMANATION (%)	PERMEABILITY MEASURED (m^2)	PERMEABILITY USSCS[a] cm/h (in./h)
Ben Lomand Nursery, Santa Cruz County	130-150 (50-60)	Residual, sandy loam (after quartz diorite) (Bowman and Estrada, 1980)	33 ± 7[b] [0.9 (±0.2)]	46000 ± 19000[c] 1252 [±519]	32[b]	7.5×10^{-13} to 4.0×10^{-11}	5.1-15 (2.0-6.0)
Las Posadas State Preserve, Napa County	76-130 (30-50)	Residual, gravelly loam (weath. rhyolite to clay) Lambert and Kashiwagi, 1978)	78 ± 7[b] [2.1 (±0.2)]	Not measurable, due to low permeability	18[b]	1.7×10^{-14} to 1.1×10^{-13}	0.5-5.1 (0.2-2.0)
Ink Grade Site, Napa County	76-130 (30-50)	Residual, gravelly loam (weath. rhyolite to clay) (Lambert and Kashiwagi, 1978)	85 [2.3]	Not measured	13	Not measured	0.5-5.1 (0.2-2.0)
Napa State Hospital	63-76 (25-30)	Alluvial, gravelly loam (Lambert and Kashiwagi, 1978)	33 [0.9]	Not measured	26	Not measured	0.5-1.5 (0.2-0.6)
Camps Parks Reservation, Alameda County	40-50 (16-20)	Alluvial, clay (Welch et al., 1966)	22[d] [0.6]	Not measured	18[d]	Not measured	0.13-0.5 (0.05-0.2)
Oxford Tract, U.C. Berkeley	50-63 (20-25)	Alluvial, clay	17 ± 30[b] [0.45 (±0.8)]	Not measurable, due to low permeability	Not measured	6.6 to 8.3×10^{-14}	No data

a   From U. S. Soil Conservation Service reports.
b   Mean of soil auger samples (11 at Ben Lomond, 9 at Las Posadas, 9 at Oxford Tract).
c   Mean of 9 measurements at 1.5, 2, and 3 m depth.
d   Based on soils of Berkeley Hills, on Orinda Formation
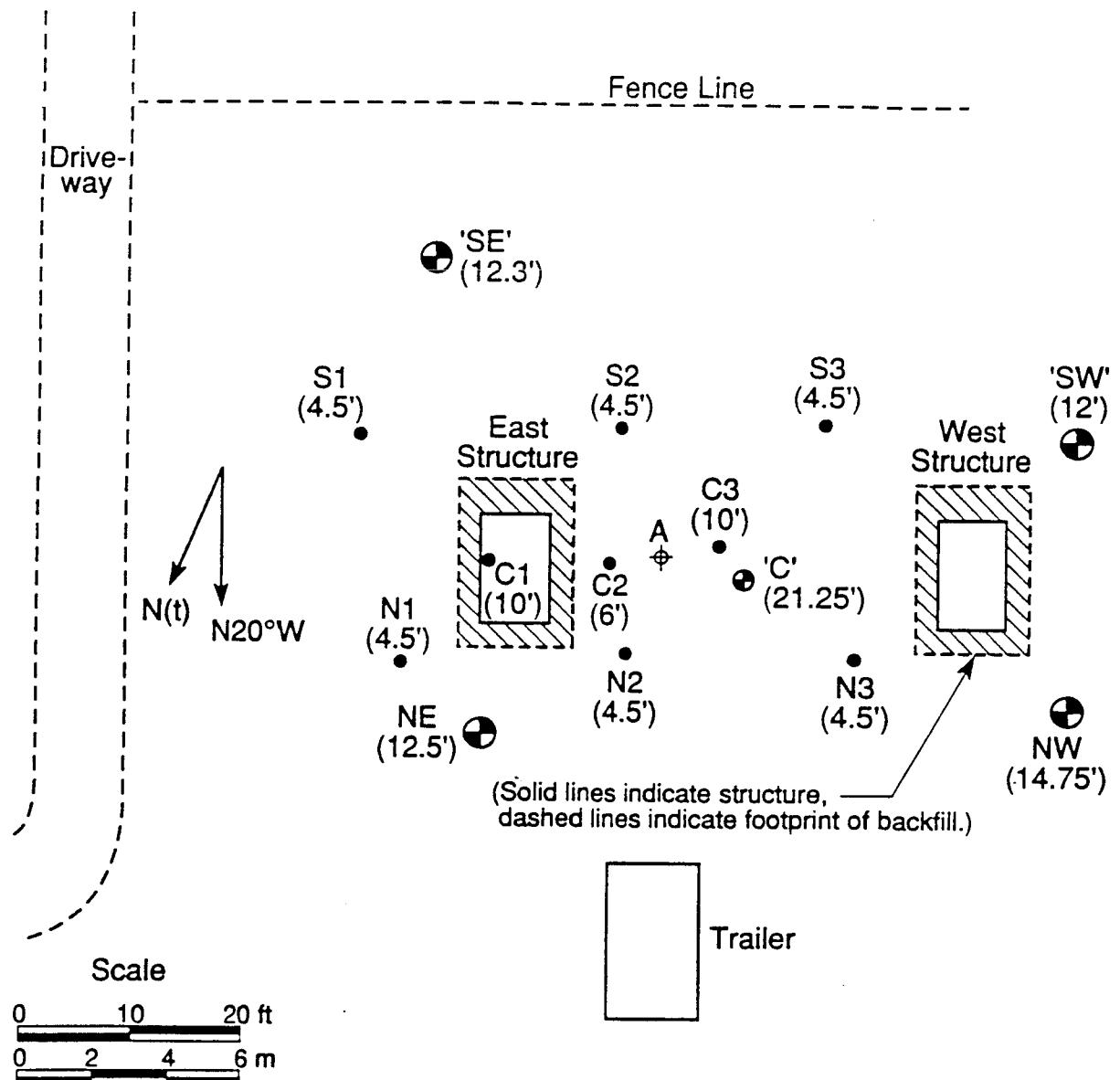
10

Table 2. Ben Lomond Site Characteristics

Soil type	Residual soil (sandy loam) developed from weathered quartz diorite[a]
Radium in soil	30–40 Bq/kg (0.8 – 1.1 pCi/g)
Emanation	28–42%
Radon in soil gas	$1.6–5.5 \times 10^4$ Bq/m^3 (600–2000 pCi/l)
Permeability (field, 9 locations)	$0.4–3.5 \times 10^{-11}$ m^2 (mean: $1.7 \times 10^{-11} \pm 1.4 \times 10^{-11}$ m^2)
(lab, 7 samples)	$0.9–6.5 \times 10^{-11}$ m^2 (mean: $2.4 \times 10^{-11} \pm 2.3 \times 10^{-11}$ m^2)
(mean)	(overall mean: $1.9 \times 10^{-11} \pm 1.8 \times 10^{-11}$ m^2)
Porosity	29–33%
Degree of saturation	49–92%
Rainfall	~150 cm/yr, seasonal
Depth to permanent water table	>4 m

[a]   Geologic setting from Leo (1967); soils description from Bowman and Estrada (1980).

39°

Coast

Great

Sacramento
☆

Pacific

LP,IG ●

Valley

N ●

38°
Point Reyes

● OT

San Francisco

●CP

San
Francisco
Bay

R
a
n
g
e
s

O
c
e
a
n

124°

BL
●

37°

Monterey
Bay

Monterey

0   50 miles

Scale

123°   122°   121°

XBL 898-7697
T.I.D. Illus. 88

Figure 1.   Location map of potential sites in the San Francisco Bay area. BL = Ben Lomond,
             CP = Camp Parks, LP = Las Posadas, IG = Ink Grade, N = Napa State Hospital,
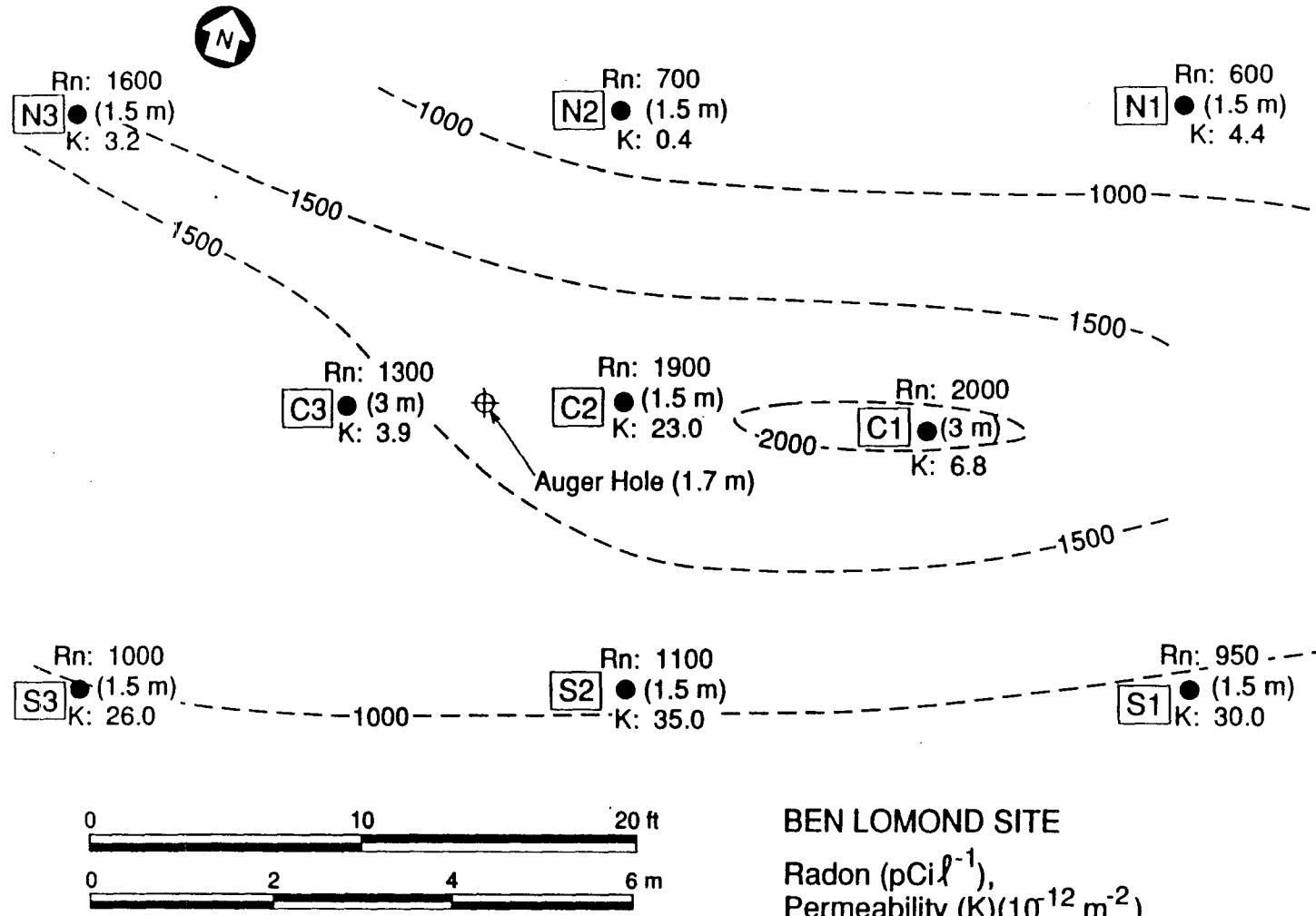   OT = Oxford Tract.

Fence Line

Drive-way

'SE'
(12.3')

S1
(4.5')

S2
(4.5')

S3
(4.5')

'SW'
(12')

East
Structure

West
Structure

C3
(10')

A

N(t)   N20°W

N1
(4.5')

C1
(10')

C2
(6')

'C'
(21.25')

NE
(12.5')

N2
(4.5')

N3
(4.5')

NW
(14.75')

(Solid lines indicate structure,
dashed lines indicate footprint of backfill.)

Scale

0   10   20 ft

0   2   4   6 m

Trailer

• Initial Rn/Permeability Probes
◕ Cored Hole
⊕ Auger Hole

Location of Principal Components
of Small Structures Project,
Ben Lomond Nursery

XBL 898-7691
T.I.D. Illus.88

Figure 2.   Layout of the Ben Lomond site, showing locations of the initial radon and
permeability measurements probes used in site selection, core- and auger holes,
and the approximate locations of the small structures. The numbers in parenthesis
indicate the depth below the local soil surface.

Rn: 1600
N3 ● (1.5 m)
K: 3.2

Rn: 700
N2 ● (1.5 m)
K: 0.4

Rn: 600
N1 ● (1.5 m)
K: 4.4

1000

1500

1500

1000

1500

Rn: 1300
C3 ● (3 m)
K: 3.9

Rn: 1900
C2 ● (1.5 m)
K: 23.0

Rn: 2000
C1 ● (3 m)
K: 6.8

2000

Auger Hole (1.7 m)

1500

Rn: 1000
S3 ● (1.5 m)
K: 26.0

1000

Rn: 1100
S2 ● (1.5 m)
K: 35.0

Rn: 950
S1 ● (1.5 m)
K: 30.0

0   10   20 ft

0   2   4   6 m

BEN LOMOND SITE

Radon (pCiℓ^{-1}),
Permeability (K)(10^{-12} m^{-2})

XBL 898-7690
T.I.D. Illus.88

Figure 3.   Spatial distributions of soil-gas radon concentrations and permeability, deter-
mined by probing during site selection, Ben Lomond site. The lines of constant
radon concentration are approximate and based on a visual inspection.
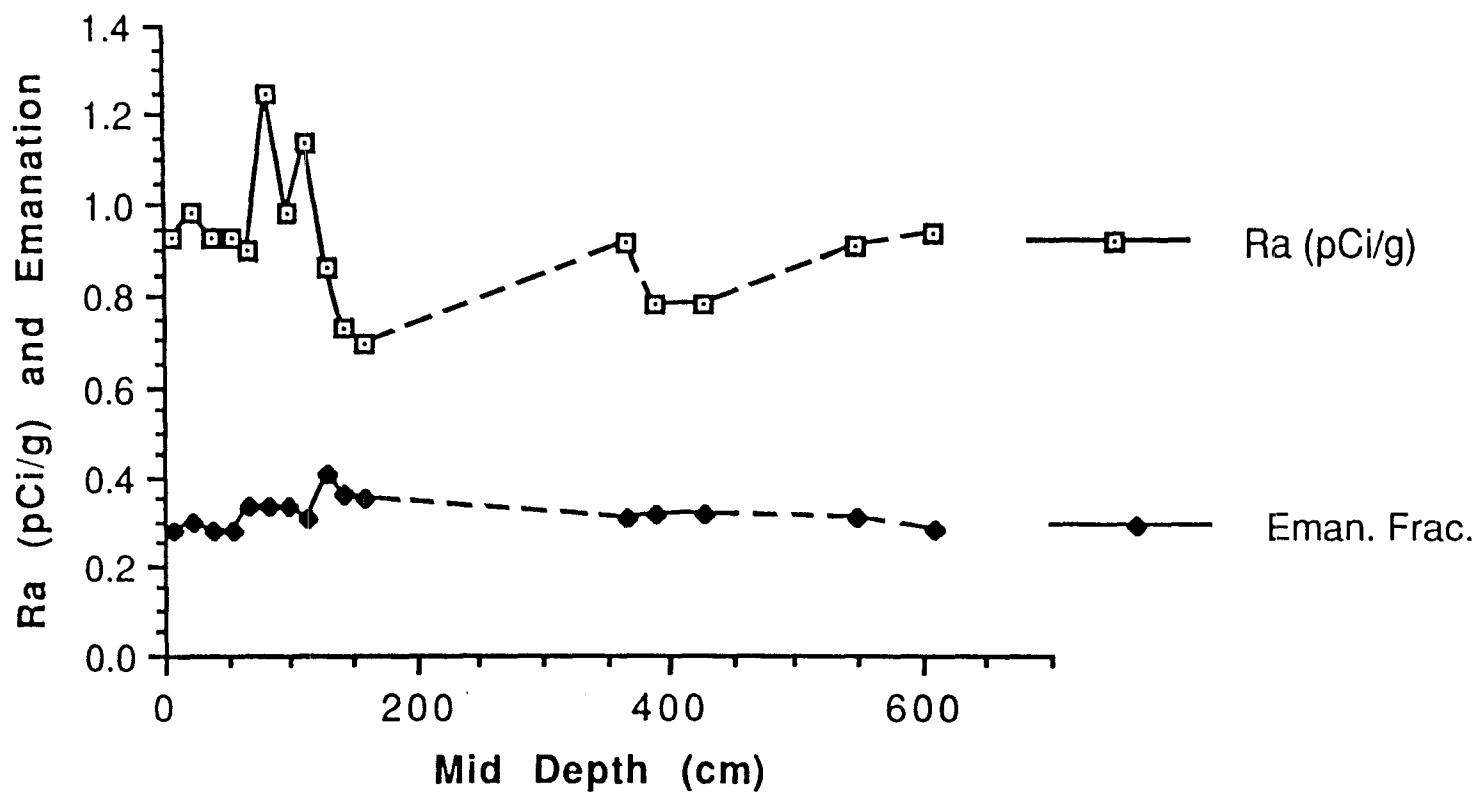
Ra and Emanating Fraction, Ben Lomond

Figure 4.   Radium concentration in pCi/g and radon-emanating fraction (dimensionless) of the soil at the Ben Lomond site as a function of depth below the soil surface.

STRUCTURE DESIGN AND CONSTRUCTION

Design Objectives

A major objective was to produce very precisely constructed structures so that uncontrolled structural features would not prevent accurate assessments of the effects of site-specific variables (e.g., soil properties) on radon entry. Consequently, we required precise control of the size and location of openings between the interior of the basements and the soil as well as a precise structure geometry. Extremely air-tight structures (~2 cm^2 total "leakage area" between the interior of the structure and outdoors) were required for two reasons. First, a small leakage area limits the rate of air leakage between the structure and outdoors, so that the structure ventilation rate is readily controlled and measured using a small mechanical ventilation system. Second, the small leakage area permits stable indoor pressure control, within the desired pressure range, by mechanically supplying and withdrawing air at different rates. In addition, with an air-tight structure at sites with a high soil permeability, soil gas entry rates can be determined (approximately) from the difference between the rates of air flow into and out of the structure because, in this situation, the soil-gas entry rate will be large compared to the uncertainty in the measured air flow rates. To simplify monitoring of backfill properties and the associated modeling, design objectives also included homogeneous soil in the backfill zone adjacent to the basement walls, with a permeability similar to that of the in-situ soil. Finally, because the initial modeling has indicated that the permeability of the soil or other material (e.g., aggregate) immediately adjacent to the exterior surfaces of the substructure has a large influence on the rate of soil gas entry, we required minimal compaction (during construction) of the existing soil beneath the basement floor and a high permeability aggregate layer beneath the floor of one structure.

Description of Structures

Room-size basements have been designed and constructed at the first site. A diagram of a cross section of a structure is provided in Figure 5. The basement floor has dimensions of 2.9 m by 1.7 m and the ceiling height is 2.3 m. The reinforced concrete floor and footing was fabricated

(concrete poured) at the site as a single unit. The floor contains six openings to the soil (1.0 m long and 0.07 m wide) around the periphery of the floor. Adjustable-width slots, consisting of parallel aluminum plates (described later), are sealed into these openings with their lower edges in contact with the soil. Additional small openings to the soil may be installed at a later date by drilling through the concrete floor or walls.

The basement walls were prefabricated of reinforced concrete and fit into a keyway formed in the top of the footing. The junction between the walls and the footing was sealed with a grout that expands slightly during hardening and with a urethane sealant. The exterior surface of the walls were sealed (water-proofed) with a polyurethane coating.
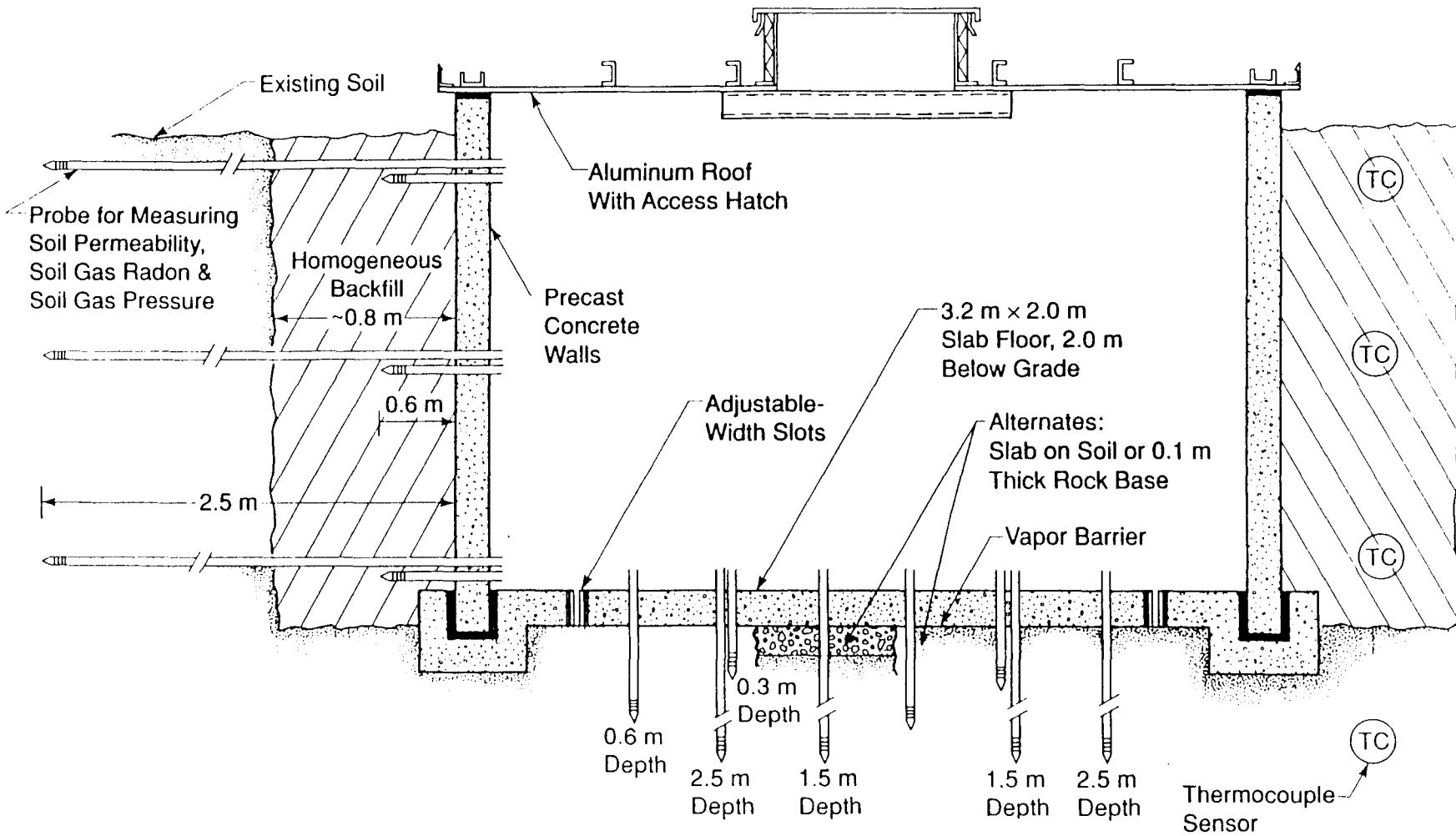
The roof was fabricated from two sheets of aluminum welded together and reinforced with aluminum channel on their upper (exterior) surface. The junction between the top of the walls and the aluminum is sealed with a gasket and caulking compound. Water that collects on the roof is directed away from the structure and surrounding soil through flexible plastic pipe. A commercially available hatch -- modified extensively to reduce air leaks and leak-tested in the laboratory -- was installed in the roof.

Wires for instrumentation and electrical power, tubing for structure ventilation and pressure control, and tubing connected to the soil probes (all originating in a trailer which houses instrumentation) enter the basements slightly below grade through electrical conduits sealed at the basement end.

The adjustable-width slots consist of pairs of precision (i.e., very flat and parallel) aluminum plates separated by precision shims, bolted together, and sealed into the openings through the slab floor. Using different sets of shims, the plate spacing (slot thickness) can be 0.13 mm, 0.64 mm, 3.2 mm, and 12.7 mm with a tolerance of approximately 0.03 mm at the smallest spacing. The assemblies of plates are sealed into the openings using a combination of flexible foam rod, duct seal, and a flowable urethane sealant designed for use with concrete. Lab tests confirmed that there is negligible leakage through this type of seal. Using a test stand in the laboratory, the relationship between flow through the slots and pressure drop has been measured and agrees with theoretical predictions within five percent.

The soil walls of the excavation were vertical and supported by shoring during construction. The region between the exterior surfaces of the concrete basement walls and the surfaces of the excavation (backfill zone) has a maximum width of 0.9 m and was backfilled with a blend of the excavated soil and compacted to achieve a relatively uniform dry density similar to the average density of the in-situ soil as described in the previous section.

The two basements at the first site are identical except one has a 0.1 m thick layer of aggregate beneath the concrete floor. The permeability of a sample of the sub-slab aggregate is being measured in the laboratory. To prevent concrete from filling any of the interstitial spaces within the aggregate or seeping into the surface of the soil (for the basement without sub-slab aggregate) and to conform with a typical house construction practice, a 0.25 mm thick polyethylene membrane was placed on the upper surface of the sub-slab aggregate or soil prior to pouring the concrete.

19

Existing Soil

Probe for Measuring
Soil Permeability,
Soil Gas Radon &
Soil Gas Pressure

Homogeneous
Backfill
~0.8 m

Precast
Concrete
Walls

0.6 m

2.5 m

Aluminum Roof
With Access Hatch

3.2 m × 2.0 m
Slab Floor, 2.0 m
Below Grade

Adjustable-
Width Slots

Alternates:
Slab on Soil or 0.1 m
Thick Rock Base

Vapor Barrier

TC

TC

TC

0.6 m
Depth

0.3 m
Depth

2.5 m
Depth

1.5 m
Depth

1.5 m
Depth

2.5 m
Depth

TC

Thermocouple
Sensor

XBL 898 6970

Figure 5. Cross-sectional view of the structures. This illustration shows pairs of closely spaced probes that are actually located one behind the other, separated by distances of approximately 0.6 m. In addition, horizontal probes extend out from all four walls in the same pattern.

MEASUREMENTS AND INSTRUMENTATION

To meet the objectives of this project, a large number of detailed measurements are required, most of which must be made on a regular basis to track the temporal variations of the parameters being studied. The variables to be monitored or controlled are described in Tables 3 and 4 and include: the radon concentration in the structure, the ventilation rate of the structure, the radon entry driving forces (temporally and spacially varying pressures and temperatures), and the structural and soil characteristics (including the locations and size of openings between the soil and the structure's interior, soil permeability to air, soil moisture content, and soil-gas radon concentration). Due to the desire to collect rapidly changing transient pressure data and the requirement of controlling indoor-outdoor or indoor-soil pressure differences, pressures will be measured on a relatively short time scale (fractions of a minute to hourly). Pressures must also be measured over a large spatial region (to map the pressure field around the structure. The soil characteristics (permeability, moisture content, temperature, and soil-gas radon concentration) will vary with time but less rapidly. In general, significant variations in these parameters will occur on an hourly to daily (or longer) time scale. These parameters are also subject to large spatial variability. To meet these data needs a flexible data-acquisition system that also controlled structure ventilation rate and the reference indoor-outdoor or indoor-soil pressure difference was required.

The types of instrumentation used to make the measurements are summarized in Table 3. The associated ranges and desired maximum uncertainties for each of the parameters are summarized in Table 4.

Although most of the instrumentation needs specified in Tables 3 and 4 are either commercially available or have been fabricated previously at LBL, the particular needs of this project push the limits of many of the measurement techniques. These demands for better instrumentation stem both from the need for long-term measurement stability, and the need to characterize a relatively large spatial region with a limited number of probes and measurement systems. The differential pressure, weather, and temperature measurements are relatively standard. The barometric pressure measurement specification required the use of a state-of-the-art pressure measurement system. Moreover, significant development efforts were needed to set up automated measurements of soil permeability and soil-gas radon concentration.

Underground Probes

As noted above, one of the principal challenges associated with the measurement needs was to characterize long-term, short-term, and spatial variabilities of the soil conditions around the structure. This is accomplished using three different types of underground probes (see Table 5).

Permeability, Pressure and Radon Concentration (Probe A)

Due to the concurrent needs to map the pressure, permeability, and radon concentration fields in the soil surrounding the structure, an all-purpose probe (called here Probe A) and associated measurement techniques were developed to monitor these three parameters. This results in three sets of design constraints for a single probe, but reduces the total number of probes required. To make accurate pressure measurements, tubing connecting the probe to the pressure transducer must either have only horizontal sections or the temperature of any vertical sections must be precisely known. For accurate permeability measurements, in addition to the requirement given above for pressure measurements, a well-defined soil/probe interface that does not change with time was required, and it was necessary to ensure that a clear majority of the measured pressure drop occurs across the soil and not within the probe. Finally, regrading radon concentration measurements, the main constraints were to minimize the internal volume of the probe to limit the soil gas required to purge the probe, and to minimize the vertical extent of the soil-volume from which a sample would be drawn. The latter of these constraints is particularly pertinent for probes near the soil surface, for care must be taken not to draw in fresh air as part of the sample.

In previous field studies, measurements of soil permeability, soil-gas radon concentration, and soil-gas pressure were made using a simple pipe as a probe. After installing these probes, a slightly longer rod with drill bit at its end was pushed through the pipe and rotated to create a small cavity at the below-grade end of the probe. This potentially imprecise "pipe-end" probe was not suitable to meet our measurement objectives.

To meet the objectives, a new type of probe was employed and installed as shown in Figure 5. This probe uses cylindrical stainless steel well screens, which are typically used to withdraw water from soil (15 cm long, 2.13 cm outer diameter), welded on one end to nominal 1/2 inch pipe (2.13 cm outer diameter) and on the other end to steel driving points. The use of a well screen, which is a hollow cylinder with slots in the walls of the cylinder, rather than a simple pipe-end

has a number of advantages for permeability measurement, including: (1) the well-screen probe measures the permeability of a much larger soil region, (2) the flow into the cylindrical well screen is less affected by the highly localized soil perturbations at the probe/soil interface, and (3) the probe/soil interface is temporally more stable for the well screen probe. The first two advantages stem principally from the fact that the isobaric surfaces in close proximity to the probe are cylindrical for the well screen, rather than approximately spherical for the pipe end, thereby reducing the relative importance of the interface and the soil directly adjacent to the interface of the well-screen probe. This effect is illustrated approximately in Figure 6, which compares the spatial regions over which 90% of the imposed pressure drop occurs for an infinitely long cylindrical probe and a perfectly spherical cavity ideally created by the pipe-end probe. To estimate the relative importance of localized soil perturbations for the two types of probes, the effect of compacting 1 mm of soil to an order of magnitude lower permeability at the exterior surface of the well screen and the interior surface of the sperical cavity was computed for an infinitely long cylindrical probe and a perfectly spherical cavity. For the spherical cavity this resulted in a 50% underprediction of the undisturbed soil permeability, versus a 15% underprediction for the cylindrical probe. The temporal stability of the well-screen probe comes from the direct contact between the soil and the screen, unlike the pipe-end probe, which has at its end a cavity of unknown (and temporally variable) size.

The well-screen probe also has an advantage over the pipe-end probe for soil-gas radon concentration measurements. For the soil-gas sampling period to be utilized, the well-screen probe allows radon samples to be drawn from a thinner vertical layer of soil, thereby reducing radon concentration variations over the course of a measurement (since radon concentrations vary with depth). This allows the uppermost horizontal probes extending from the walls of the structures to be placed closer to the surface. The diameter of the probe was based on minimum size limitations for the well screens available. Smaller diameter probes would both reduce edge effects on the cylindrical geometry for permeability measurements, and reduce purge time for radon concentration measurements. However, the inner diameter of the probe (approximately 1.5 cm) could not be reduced indefinitely due to the increase in flow resistance associated with decreases in diameter.

Most probes were installed horizontally, passing out of the structure through walls, and thereby not requiring any vertical sections of tubing between the probe and pressure transducer. The seven depths correspond to: (1) 25 cm below the soil surface, (2) mid-depth of the wall, (3) slab depth, and (4) four different depths below the slab (as shown in Figure 5). The horizontal probes were installed at two distances from each side of the structure, one in the backfill zone near the structure, the other approximately 2 meters from the wall. Vertical sections of probe were obviously required for the below-slab probes. The eight below-slab probes are located between 0.17 and 2.3 meters below the slab. There is one additional horizontal probe (not shown in Figure 5) used by the pressure control system to reference the structure pressure to a region which is effectively uninfluenced by the structure (approximately 6 meters from the structure near the level of the slab floor).

Soil Moisture (Probe B)

Soil moisture content is of importance to the project for three reasons: (1) it affects the gas permeability of the soil by altering the pore spaces, (2) it affects soil-gas radon concentration due to changes in radon enamation and gas transport, and (3) temporal changes in soil moisture can create spatial pressure variations which can alter soil-gas entry rates and routes. To take into account all of these effects, and to assure long-term measurement stability, an apparatus which has only recently become commercially available will be employed, although it has not yet been received from the vendor. This apparatus implements Time Domain Reflectometry (TDR) to obtain the moisture content from the pulse reflected by two waveguides implanted in the soil. The technique is based upon the change in dielectric constant of soil associated with a change in soil moisture content. The moisture content will be monitored at four depths for two locations, one in the backfill region, the other in undisturbed soil. The four depths are: (1) 20 cm below the soil surface, (2) mid-depth of the wall, (3) slab depth, and (4) just below the slab. The waveguides, which consist of 30 cm long stainless steel rods spaced 5 cm apart, are mounted at the ends of vertical plastic pipes of appropriate lengths. The signal cables from each pipe are all connected to a switch that multiplexes the different probes to a single TDR signal generator and data logger.

Soil Temperature (Probe C)

Soil temperature profiles are monitored primarily to examine the potential importance of buoyancy-forces on soil-gas flows and radon entry, and determine the contribution of soil gas temperature variations to the basement/soil pressure differentials. To meet these needs, thermocouples were inserted in two vertical plastic pipes, one in the backfill region, the other in the undisturbed soil. Each pipe has four thermocouples, located at approximately the same depths used for the other probes: (1) 15 cm below the soil surface, (2) mid-depth of the wall, (3) slab depth, and (4) below the slab. Vertical heat conduction within the pipes was minimized by filling the pipe with dry sand and sealing the top after thermocouple installation.

Radon Concentration Measurements

Accurate radon concentration measurements at three types of location: within the structure, at the radon entry location, and within the soil, are key to meeting the objectives of this project. As such, considerable care was needed to develop radon concentration monitoring protocols. Soil-gas radon concentration measurements posed the most significant difficulties because of the need to monitor numerous locations with a limited supply (due to high cost) of Continuous Radon Monitors (CRM). Therefore, soil-gas samples from different soil locations (Probe A) are multiplexed through a single CRM, making it imperative that the time period required for withdrawing and analyzing a given sample be as short as possible. The frequency at which samples could be analyzed was increased by minimizing the flush time between samples. This is accomplished by counting (i.e., measuring the radon concentration of) a given sample while flushing the next probe (and associated tubing) with a soil gas sample to be counted. Due to the deposition of radon daughters (with time constants for radioactive decay comparable to the desired sampling periods) on the walls of the scintillation cell within the CRM, a dynamic calibration and measurement protocol that takes into account the deposition and decay of daughters was needed (Busigin 1979). To arrive at the appropriate compromise between measurement period and measurement uncertainty, the uncertainty associated with each measurement had to be determined as a function of measurement period. Also, due to the wide range of soil-gas radon concentrations, the measurement history has a significant impact on the uncertainty associated with a given measurement. The order in which different locations are sampled is important. The sampling protocol adopted is illustrated in Figure

7 and incorporates a staircase ascent from outdoor air to the highest concentration, followed by a staircase descent to outdoor air (approximately zero concentration, which provides information on background count rates of the scintillation cell). The uncertainty associated with this and other protocols is presently being quantified both with laboratory measurements, and with Monte Carlo simulations. The results of laboratory-based measurements of radon concentrations with and without corrections using the Busign (1979) procedure, are shown in Figure 7. In addition to these efforts, a modified dynamic model for analyzing CRM data, which uses a variable analysis timestep to reduce total sampling time, and x^2 minimization to improve measurement uncertainty, is being examined.

Another incentive for minimizing the required sampling period for a given probe, and another constraint on the sampling order, stem from the effects of withdrawing CRM samples from the soil on soil pressure and radon fields. For example, the standard 200 cc/min flow through a CRM has to be compared with flows of soil gas into the structure between 10-10000 cc/min. For all probes, but especially for those near the surface, the longer the sampling time, the larger the temporal variation in radon concentration over the course of a measurement. As far as the sampling order is concerned, it is important to assure that the soil-gas flows created by a given measurement do not significantly affect subsequent soil-gas concentration measurements.

In addition to the CRM measuring soil-gas radon concentration, there are two other CRMs, one to measure the radon concentration of the air in the structure, and one to measure the average concentration of the incoming soil gases by withdrawing a sample from multiple locations in the openings to the soil. Both of these devices were calibrated dynamically, i.e., with time-varying radon concentrations, so that the Busign (1979) procedure can be used; however, a high measurement frequency is less important for these measurements. On the other hand, the CRM used to monitor incoming soil-gas concentration must be operated at a very low sample flow rate and sample via a manifold so as not to disturb the flow into the structure. Finally, the background count rate (due to deposition of long-lived decay products on the cell walls) of all CRMs will be checked periodically.

Data Acquisition and Control

An IBM-AT compatible computer with plug-in I/O cards was chosen for the data acquisition system. The choice of such a system made it possible to use commercial multi-tasking data acquisition software, and provided a large inexpensive on-site data storage media (70Mb hard disk) as well as straightforward modem communication for transferring data to computers at LBL. The structure of the data acquisition software allows for several independent, remotely-programmable tasks, including: (1) control of pressures in the structure, (2) continuous routine data acquisition, (3) periodic measurements of permeability, soil-gas radon and soil moisture, and (4) various short-term transient tests. The pressure control task will implement a PID Control loop for the rate of flow of exhaust air from the structure, thereby controlling the pressure differential between the structure and the far-field soil-gas pressure (or, in some experiments, between the structure and the pressure at the soil surface). The control will be accomplished by driving a Mass-Flow Controller (MFC) based upon the measured pressure differential. An additional control loop will control the ventilation rate of the structure based upon the remotely-programmable flow rate through a second MFC connected to an intake (air supply) pump. Continuous data acquisition of specific parameters, which include pressure, temperature and weather measurements, can take place at any frequency lower than 10 Hz.

Periodic permeability, soil-moisture and soil-gas radon tests will be based upon multiplexed sensors. Although the soil-moisture measurements can be extremely quick, the frequency of permeability and radon concentration measurements will be limited. Soil-gas radon will have the longest cycle times, at present no faster than 5 minutes per sample point (i.e., the 32 samples around a structure require more than 2.5 hours). The cycle time for permeability measurement falls somewhere between these two. To make up for cycle-time limitations, the routine data acquisition includes more frequent measurement of permeability and radon concentration at selected locations. Transient tests will have the same frequency limitations for permeability, soil-moisture and soil-gas radon, however the soil-gas pressures, even though they are multiplexed, will have a cycle time of about 10 seconds.

Table 3. Variables and instrumentation

| Variables	Instrumentation
Pressure differentials	Electronic Pressure Transducer
Temperatures	Thermocouples
Weather	Aspirated Thermocouple, Cup Anemometer, Tipping Bucket Rain Gauge, Electronic Barometric Pressure Transducer
Soil moisture	Time-Domain Reflectometer
Soil permeability	Electronic Pressure Transuducer plus Mass-Flow Controller
Radon concentrations	Continuous Radon Monitor
Air flows	Mass-Flow Controllers

Table 4. Parameter ranges and desired maximum uncertainties

Parameter	Range	Target Maximum Uncertainty
Differential pressure	0 - 100 Pa	0.1 Pa
Barometric pressure	0.96 - 1.06 × 10^5 Pa	1 Pa
Temperature	-20°C - 40°C	0.5°C
Windspeed	0 - 20 m/s	0.3 m/s
Precipitation	0 - 5 cm/h	0.1 cm/h
Soil moisture content	0 - 0.6 m^3/m^3	0.03 m^3/m^3
Radon concentration	> 20 Bq/m^3	10% (above 200 Bq/m^3)
Ventilation air flows	5 - 50 l/min	0.5 l/min
Parameters to determine soil permeability		
Soil-gas flow through probe (from site to site)	0.002 - 2 l/min	5%
Imposed pressure at probe (at a given site)	10 - 100 Pa	0.1 Pa

Table 5.   Underground probes to characterize surrounding soil conditions.
Probe locations are illustrated in Figure 5.

Probe	Variables	Depths	Total Number of Locations
A	Permeability, Pressure, Radon concentration	7	32
B	Moisture content	4	8
C	Temperature	4	8

Spherical probe
with diameter D;
90% of
pressure drop
in sphere of soil
with diameter 8 D
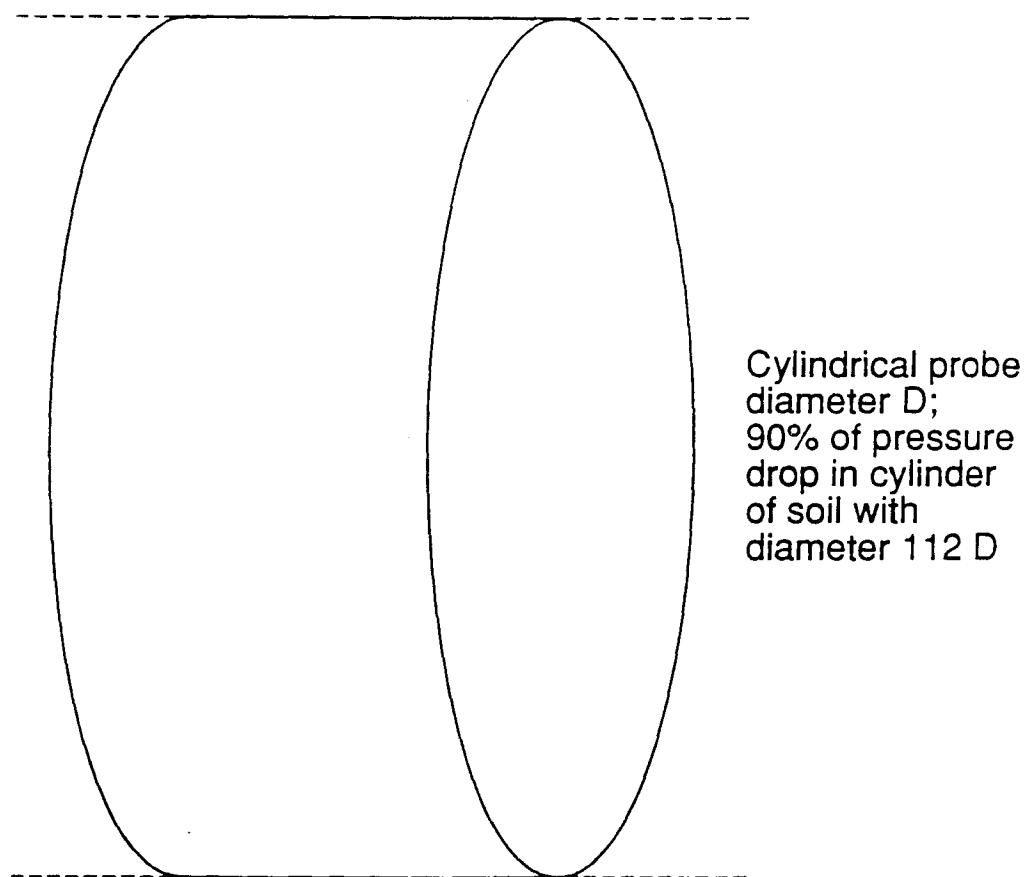
Cylindrical probe
diameter D;
90% of pressure
drop in cylinder
of soil with
diameter 112 D

XBL 899-6282

Figure 6.   Illustration of the volumes of homogeneous soil that account for 90% of the total pressure drop due to flow through ideal perfectly spherical and infinite-cylindrical probes used to measure soil permeability. The soil volumes shown in this figure are based on an infinite, rather than semi-infinite, soil region.

Laboratory Test of Radon Concentration Tracking

time [minute]

```
........ Actual Radon Concentration
———— Uncorrected Radon Concentration
········ Corrected Radon Concentration (Busigin)
```
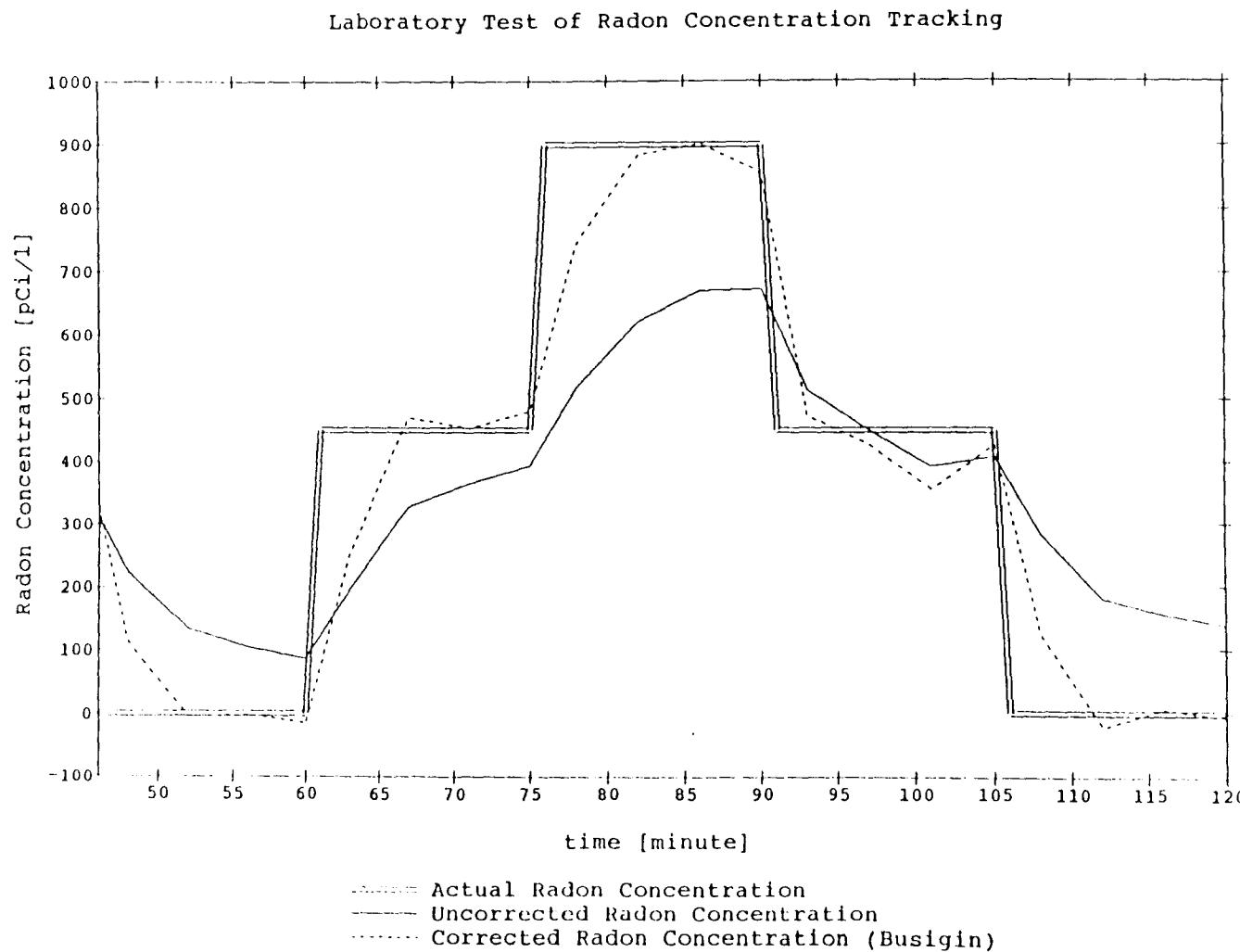
Figure 7.   Comparison between actual time-varying radon concentration and the concentration predicted using continuous-radon-monitor data with and without data correction using the Busigin (1979) method.   In actual practice, radon concentrations are determined by averaging the predictions during each measurement period, excluding the first few predictions which are affected by purging the scintillation cell of the previous sample.

EXPERIMENTAL PLANS

To lay the groundwork for our discussion of experimental plans, we first identify the major parameters that drive or otherwise control the radon transport process. These parameters include site specific soil characteristics (soil permeability, soil radium concentration, radon emanating fraction) which may vary spatially at the site, and "naturally" varying parameters including soil moisture, soil and outdoor temperatures, barometric pressure, wind speed, and precipitation, which are affected by weather. In addition, some parameters are subject to our direct control: the indoor-outdoor or indoor-soil pressure difference, the location and size of openings to the soil, and the option of placing aggregate beneath the slab floor (present beneath the floor of one structure). We also identify a group of intermediate measured variables and primary measured results that vary in response to the "controlling parameters" noted above. These variables are the soil gas pressures, soil gas radon concentrations, soil gas entry rate, concentration of radon in the entering soil gas, and radon entry rate. Our experimental plans at each site are designed primarily to examine the relationships between the controlling parameters and the intermediate and final measured variables. The experiments are designed to provide a more thorough understanding of the mechanisms of radon entry and the relative importance of the different controlling factors. In addition, the experiments will provide data of sufficient quality and detail to allow model validation. Simultaneously, we will obtain information on the variations in critical soil properties (e.g., permeability and soil gas radon) with soil moisture and over time.

The impact of site-to-site differences in soil conditions on radon entry and on the other measured variables will be determined by comparing the data obtained from identical structures and operating conditions at the different sites. Similarly, the effects of subslab aggregate will be determined via a comparison of the data from the two different structures located at the same site in a region with relatively homogeneous soil.

At each site, our plans include cycling between a number of different methods of controlling the indoor-outdoor pressure difference while other controlling parameters vary naturally (e.g., soil moisture) or intentionally (e.g. slot width). The duration of the operational cycles will be approximately one week. The following paragraphs describe the methods of pressure control and the motivation for the various control methods.

In one mode of pressure control, where confounding factors are minimized, the indoor-outdoor pressure difference will be maintained constant with the outdoor reference pressure at a point within the soil at slab floor level and sufficiently distant from the structure to be substantially unaffected by the flow through the soil. In this mode, the pressure difference that drives radon entry will be essentially constant despite variations in atmospheric pressure. The indoor-outdoor pressure difference will, in some cases, be maintained above the typical level in houses in order to increase the magnitude (and thus increase measurement accuracy) of some parameters such as soil gas pressures.

In another control mode, the indoor-outdoor pressure difference will again be maintained constant but the reference outdoor pressure will be at the soil surface. The driving force for radon entry will, in this case, be influenced by variations in atmospheric pressure and time lags in soil gas pressures. We may find evidence of temporal variations in radon entry rates and/or pumping of soil gas/indoor air into and out of the basements through the penetrations to the soil.

We also plan at least two types of transient experiments. In one case, the indoor-outdoor pressure difference will be changed abruptly (i.e., step change) and data will be collected rapidly as the measured parameters (e.g., soil-gas pressures, soil-gas radon concentrations, and radon entry rates) respond to this step change. In another control mode, the indoor-outdoor pressure difference will be varied in a periodic (e.g. sinusoidal) manner, for example, to simulate barometric pressure variations or diurnal variations in pressure difference due to daily changes in the indoor-outdoor temperature difference. We expect to obtain information on the time lags, phase shifts, and damping of the measured parameters. In addition, the transient data will provide more accurate information on the extent to which the soil gas flow affects certain measured variables. Transient data are also required to validate transient models.

In yet another mode of operation, designed primarily to investigate the importance of buoyancy forces on soil gas flow, we will raise the temperature within the structure substantially (e.g., 20 C) above soil temperatures for a sufficient period to raise soil-gas temperatures near the substructure. At other times the indoor temperature will be maintained constant but only slightly above the soil temperature to limit buoyancy forces caused by heat loss from the structure to the surrounding soil. The data from the two periods will be compared. With the elevated indoor temperature, the

indoor-outdoor pressure difference will be maintained constant using the mechanical ventilation/pressure control system or, at other times, allowed to float naturally. When the indoor-outdoor pressure difference floats, we expect to obtain information that helps to explain diurnal variations in indoor radon concentrations.

We should encounter periods of heavy rainfall during some of the experimental cycles. One hypothesis, based on data from field studies, is that the downward flow of water through soil tends to push soil gas and radon into substructures. Our data will permit an evaluation of this hypothesis.

The structures also provide us with a unique, well-characterized setting to test proposed "diagnostic techniques" designed primarily to obtain information at housing sites. For example, we will evaluate methods of assessing the characteristics of subslab materials (e.g., soil or aggregate) through the use of probes and by simultaneously controlling indoor pressures. In addition, diagnostic techniques aimed at obtaining estimates long-term-average indoor radon concentrations can also be evaluated at the structures. Finally, the structures are also suitable for detailed investigations of radon control techniques.

MODELING OBJECTIVES AND PLANS

Modeling is a second major thrust of the project. In terms of understanding the results of the experiments and predicting their implications for other, more varied situations, a model is essential. While experimental investigation forms the basis on which one has confidence in a model, experiments are expensive and time-consuming, and not possible for every situation. Whenever possible, models should be verified by comparing predictions with observations for a limited number of data points spanning the range of governing variables.

This role of models in interpretation of experimental data takes on greater importance in the present case because it is not easy to intuitively develop a quantitative understanding of the transport of soil-gas and radon into basements. Although the basic physical principles of the disparate phenomena that participate in the process are understood reasonably well, their interplay is too complex to be quantified by simple calculations or even with sophisticated analytical methods. These analytical methods usually apply only for situations with rather simple (and often unlikely) assumptions about such features as boundary conditions, homogeneity, and relative importance of

competing effects. Only with numerical models incorporating the various diverse physical processes can one hope to gain an understanding of the full complexity of soil-gas and radon transport in soil and their entry into buildings.

The models have been used to guide aid the design of instrumentation and experimental configuration by making available quantitative estimates of various sub-processes. One of the crucial tasks in the present project is to test the predictions of the existing models by supplying them with some of the experimental data, and comparing predictions to observations of other datapoint values. The experiments will thus help validate some of the range of model applicability.

Early modeling efforts for the radon entry problem can be traced to Scott (DSMA 1983 and 1985). Soil-gas and radon entry rates into a house, driven by stack-effect and wind-induced pressure differences, were modeled using two-dimensional finite difference and finite element models. The purpose was to investigate the dependence of radon entry rate on various site and construction factors. Scott's efforts were followed by a more detailed two-dimensional numerical model of soil-gas entry through homogeneous soil by Mowris and Fisk (1988), who showed that their numerical predictions of entry rate of soil-gas through perimeter cracks in concrete slabs were comparable to the approximate analytical predictions obtained for the rate of soil-gas flow into buried horizontal cylinder in a semi-infinite homogeneous soil. Loureiro (1987) developed a model based on the Patankar-Spalding algorithm for two- and three-dimensional transport of soil-gas and radon (through soil with some heterogeneous features) into a house having a basement with one perimeter crack. Garbesi and Sextro (1989) used a finite element model to study soil-gas transport through soil with layers of different permeability and into basements constructed with permeable concrete block walls. These models did not simulate buoyancy forces and were confined to steady-state flow. More recently, the Loureiro code has been further developed by Revzan et al. (1989) for the current research project as discussed in the next section. This category of models is usually confined to an orthogonal coordinate system (e.g., rectilinear Euclidean, or cylindrical), and so far, has not been extended to transient flow simulations. The advantages of these models are their relative simplicity and adaptability. The disadvantages are the requirement of large computer memory and time to obtain high spatial resolution (owing to large numbers of grid nodes being generated in unessential places from the rectilinearity of the coordinates), the resulting slow execution speed, and also the fact that these models did not have transient modeling capability or,

35

before this project, incorporate the effects of buoyancy on the soil-gas transport. The predictions from these models (in the absence of a diffusion mechanism) have been successfully compared with those from exact analytical solutions for the steady-state radon transport in bipolar coordinates. (Analytical solutions in the presence of diffusion are not available, so this is the best available analytic comparison that we have).

The second line of modeling stems from the substantial effort from LBL's Earth Sciences Division in modeling of underground transport processes. The earlier modeling was based on the work by Edwards (1969) which was considerably enhanced by Narasimhan (1975). These models are based on an integrated finite difference method which allows great flexibility in coordinate density and resolution and, thus, in modeling of heterogeneous soils and complex geometries. The models were initially developed for studying deep underground flows and already incorporate compressibility and transient flow modeling capability. Simultaneous liquid (water) and gas transport can be modeled. Bouyancy forces will be added in the course of the present project.

A third direction has been the primarily analytical modeling work of Nazaroff (1988). His approach is limited to bipolar coordinates which allow modeling of soil-gas entry in a long depressurized horizontal cylindrical cavity in a homogeneous semi-infinite soil. The cylindrical cavity in the model can be used as a good approximation to a crack in the basement. The model ignores diffusive transport of radon to obtain analytically tractable equations.

The modeling effort for this project has the following primary goals: (1) to verify the adequacy of the various sub-models for simulation of soil-gas and radon transport process and to develop additional capabilities as needed, and (2) to assess the importance of various transport mechanisms (e.g., buoyancy-driven flow, barometric "pumping" of soil gas into basements), and site and building construction parameters, based on parametric simulations.

STEADY-STATE NUMERICAL MODELING

The Numerical Model

For the steady-state numerical modeling we employ a numerical model originally due to Loureiro (1987), which is in turn based upon widely accepted techniques described by Patankar (1980). The

full model comprises three independent steady-state difference equations, which are solved by computer for the temperature, pressure, and radon concentration fields in a volume of soil surounding a house with a wholly or partially sub-surface basement. From the velocity of soil gas and the radon concentration, we are able to compute the mass transport of radon at any point. The original computer code was based on a rectangular coordinate system; however a code for cylindrical coordinates has been developed for this project. Both codes are written in Fortran. In the cylindrical version, axial symmetry is assumed, so that the problem is effectively two-dimensional, permitting more rapid solutions to be obtained on small computing systems. This version, which solves the complete model, runs on any VAX computer using the VMS operating system. In the rectangular version, we assume symmetry across the two vertical planes through the center of the house, so that the problem can be limited to one quadrant of the basement-soil system. Currently, this version provides only the pressure and concentration fields; it is fully portable, apart from the usual system-dependent input/output instructions, but it is designed to run on a Cray.

In a typical problem, the boundaries are the walls and floor of the basement, the surface of the earth outside the basement, and artificial boundaries some distance beyond (horizontal-, e.g., r-direction) and below (z-direction) the basement. If it is desired to determine the radon entry rate without considering the effect of nearby houses, the outer boundaries of the soil block are chosen on the basis of parametric runs so that further expansion of the soil block produces negligible changes in results; otherwise, the boundary in the r-direction is fixed at one half the assumed distance between houses, which, due to symetry (if the houses are identical), is approximately a no-flow boundary. The basement shell may have one or more openings of arbitrary width. The cylindrical code requires that the opening be cylindrically symmetric; the rectangular code permits rectangular openings of any size, but there must be a similar opening in each quadrant.

The basic equations that underlie the model are introduced briefly in the subsequent text. The difference equation for the temperature field is a discrete expression of the differential equation

$$\nabla \cdot (K \nabla T) = 0 \tag{1}$$

where T is temperature and K thermal conductivity, which may vary from point to point. This is a valid equation for the temperature field since conductive heat transfer in the soil (away from openings to the basement) is approximately 10^5 times greater than convective heat transfer due to soil gas movement. This equation is solved numerically with Neumann boundary conditions at r

= r_{max}, i.e., we assume that an identical neighboring house operates at the same temperature so that no heat flows across the dividing line between the two houses. At $z = 0$, $z = z_{max}$, and at the inside of the basement, we employ Dirichlet conditions, i.e., the temperature is fixed, for example, at 15 C for the basement, 10 C for the soil at depth z_{max} and 0 C for the soil surface, to represent winter conditions. The thermal conductivity of the soil, which is a function of moisture content, is taken to be half that of the concrete basement shell; a change in this ratio does not alter the results materially. Boundary conditions at openings in the shell do not figure in the calculation of the temperature field.

The difference equation for the pressure field is a discrete expression of the differential equation

$$\nabla \cdot (\rho \vec{v}) = 0, \tag{2}$$

where ρ and $\vec{v}$ are, respectively, the density and bulk (volume-averaged, i.e., not pore) velocity of the soil gas. We employ the typical Boussinesq approximation, i.e., we assume that the density in Equation 2 is constant. The velocities are calculated with the equation

$$\vec{v} = -\frac{k}{\mu}(\nabla P - \rho g \hat{z}), \tag{3}$$

where P is pressure, g is the acceleration of gravity, $\hat{z}$ is a unit vector in the z-direction, taken positive into the earth, k is permeability, μ is the viscosity of soil gas (i.e., air), which has been assumed independent of temperature, and ρ is the soil gas density, which is dependent on the previously calculated temperature. The boundary conditions are Neumann (i.e., the normal velocity vanishes) everywhere except at the surface of the earth, at which the pressure is taken as atmospheric, and at the openings in the shell, where an exact solution is used to obtain the pressure at the soil surface on the basis of an assumed basement pressure.

Finally, the difference equation for the radon concentration field is a discrete expression of the differential equation

$$\vec{v} \cdot \nabla C = \nabla \cdot (D \nabla C) + \epsilon (S - \lambda C), \tag{4}$$

where $\vec{v}$ is the previously calculated velocity, C is the concentration, D is the bulk diffusivity of radon in soil, λ is the radon decay constant, ϵ is the porosity of the soil, and S is the rate of radon generation per unit volume of soil. The boundary conditions are Neumann everywhere save at the

surface of the earth, where C=0, and at the openings in the shell, where an exact solution of the equation for the concentration in the crack (Loureiro, 1987) is used to obtain the concentration at the soil.

In all cases, a variable grid spacing is used, the grid becoming more dense where large changes in the field are expected, e.g., at the openings. The difference equations are solved iteratively until certain conditions are met. Normally, we require that the largest change in the normalized temperature, pressure, and concentration fields from one iteration to the next be less than 10^{-6}. We also require that the velocity and flux of radon at the openings meet a similar condition.

Comparison with an Exact Solution

Simple analytic solutions have, of course, been used to validate the solution techniques, but there is no analytic solution available to verify the full model. The closest approach to a solvable model is the simple bipolar solution discussed by Mowris and Fisk (1988) and by Nazaroff (1988). In the solvable model, a horizontal cylindrical cavity of infinite length at pressure p_0, lies in a homogeneous semi-infinite medium below a plane at pressure zero. The cylinder may be used to represent (approximately) a crack at the junction of the basement walls and floor if the origin of the bipolar system is at the center of the crack. We expect the rates of flow into the cylindrical cavity and into the wall-floor crack to have essentially the same dependence on soil permeability and pressure difference. However, the bipolar solution does not account for the presence of the basement in the soil. The basement obstructs some of the flow path and, thus, reduces the flow. Therefore, to obtain correspondence between the bipolar and numerical predictions, the rate of flow into the cavity must be reduced by some constant factor with a value below unity (approximately 0.5 considering the geometry).

In Figure 8, we compare the analytic solution of the mass transport equation without diffusion in bipolar coordinates to results of the numerical model using the assumptions of homogeneous soil, vanishing diffusivity, no resistance to flow in the crack, no footer at the base of the walls, uniform soil temperature, and a single peripheral opening of width 0.003 m in the floor adjacent to the wall. In each case, the pressure at the opening is -5 Pa, referred to the pressure at the surface; this value is typical of pressures occurring in basements during cold weather (Revzan,

1989). The entry rate has been normalized by dividing by the soil-gas radon concentration at a great distance from the basement and the soil surface to obtain an entry rate that is independent of the soil radium concentration and radon emanating fraction. Because the bipolar solution is two-dimensional, we also normalize the entry rate to a 1 m opening length. In the bipolar solution, the cylinder center is at 2.15 m depth. In the numerical model, the basement is of radius 5 m, and has a floor of thickness 0.15 m located 2 m below the surface. The boundaries of the soil block are far enough from the basement that negligible additional flow results from their further extension. The predicted radon entry rates of the two models agree well when the entry rate predicted using the bipolar solution is multiplied by 0.375, which is consistent with expectations.

Results

Many results of interest are given in Loureiro (1987). We describe here, in summary, additional results which have been obtained after necessary alterations of the numerical model. There are two principal avenues of research which our work has been designed to explore: first, in connection with the previously described controlled experiments on radon entry, in which sites must be modelled closely, it has been necessary to increase the flexibility of the model in handling soil inhomogeneities and structural features; second, our interest in understanding the statistical distribution of indoor radon concentrations has led us to compare the predictions of the model with measured entry rates and to consider broadly the influence of soil permeability and structural features on radon entry into basements. We are presently preparing two papers in which these subjects will be covered in detail.

As originally written, the model permitted the soil permeability, the diffusivity of radon in soil, the porosity of the soil, the radon concentration of the soil, and the radon emanation coefficient of the soil (i.e., the fraction of the radon produced in the soil granules that actually enters the pore spaces) to vary from point to point, but it did not permit the user to define regions with differing characteristics with any facility. We have corrected this, and we have focussed on the following five regions of interest: first, the area immediately under the basement slab, which is often a layer of high-permeability gravel placed by the builder; second, the impermeable concrete mass supporting the basement walls, called the footer; third, the region of disturbed soil (backfill zone), between

the basement walls and the undisturbed soil; fourth, layers of high permeability in otherwise homogeneous soil; fifth, areas of high permeability which extend from the opening in the basement to the surface, allowing a preferred path for soil gas transport. Similarly, the original model did not permit more than a single opening in the basement shell, nor did it permit the opening to be situated anywhere but at the wall-slab junction. We have modified the model to allow openings of any size to be placed anywhere in the shell and have studied the influence of position on the radon entry rate.

Figure 9 shows the effect on radon entry of sub-slab gravel layers of various permeabilities for otherwise homogeneous soils of four different permeabilities. The entry rate is normalized by the soil gas radon concentration as described previously. The influence of the permeability of the gravel layer on radon entry is clearly considerable, particularly when the bulk of the soil is of low permeability. Among other results of interest, which lack of space precludes illustrating, are the following: the presence of the footer has only a minor effect on radon entry, except when circumstances are such that much of the soil gas flow occurs very near the basement walls; soil layers of relatively high permeability are of limited importance in many situations, but channels of high permeability extending from the opening in the basement shell to the soil surface have great significance; the position of the opening, so long as it is in the floor slab, is of little importance, but openings in the wall can actually reduce radon entry by providing a preferred path for soil gas that is low in radon.

We have shown (Revzan et al. 1989) that the model, with our addition of terms to account for buoyancy effects on soil-gas flow, predicts radon entry rates which are 25% lower than the mean of those measured in the winter in houses with basements in the Spokane River Valley of Washington and Idaho. We have also shown that the difference between prediction and measurement may be accounted for by inaccuracies in the measurement of soil permeability or by assuming that certain inhomogeneities exist at the sites of the houses. We have also shown that lognormally-distributed soil permeabilities (distributed among geographic regions), with a large geometric standard deviation (GSD), are consistent with measured lognormally-distributed indoor radon concentrations in houses with basements, even though the GSD of the this distribution of radon

41

concentrations is much smaller. Figure 10 illustrates the dependence of normalized radon entry rate on permeability with and without thermal expansion (buoyancy effects) and with the presence of sub-slab gravel of two permeabilities.

Finally, we have investigated the importance of the so-called "crack resistance", which becomes the factor limiting the radon entry rate when the soil is of very high permeability. For our standard opening width of 0.003 m, the crack resistance reduces the radon entry rate by no more than 10% for soil permeabilities within the range of those expected for building sites. For an opening of 0.001 m, however, the effect of crack resistance is significant at much lower soil permeabilities, so that the radon entry rate for a given house may depend substantially on the nature of the cracks in its basement.
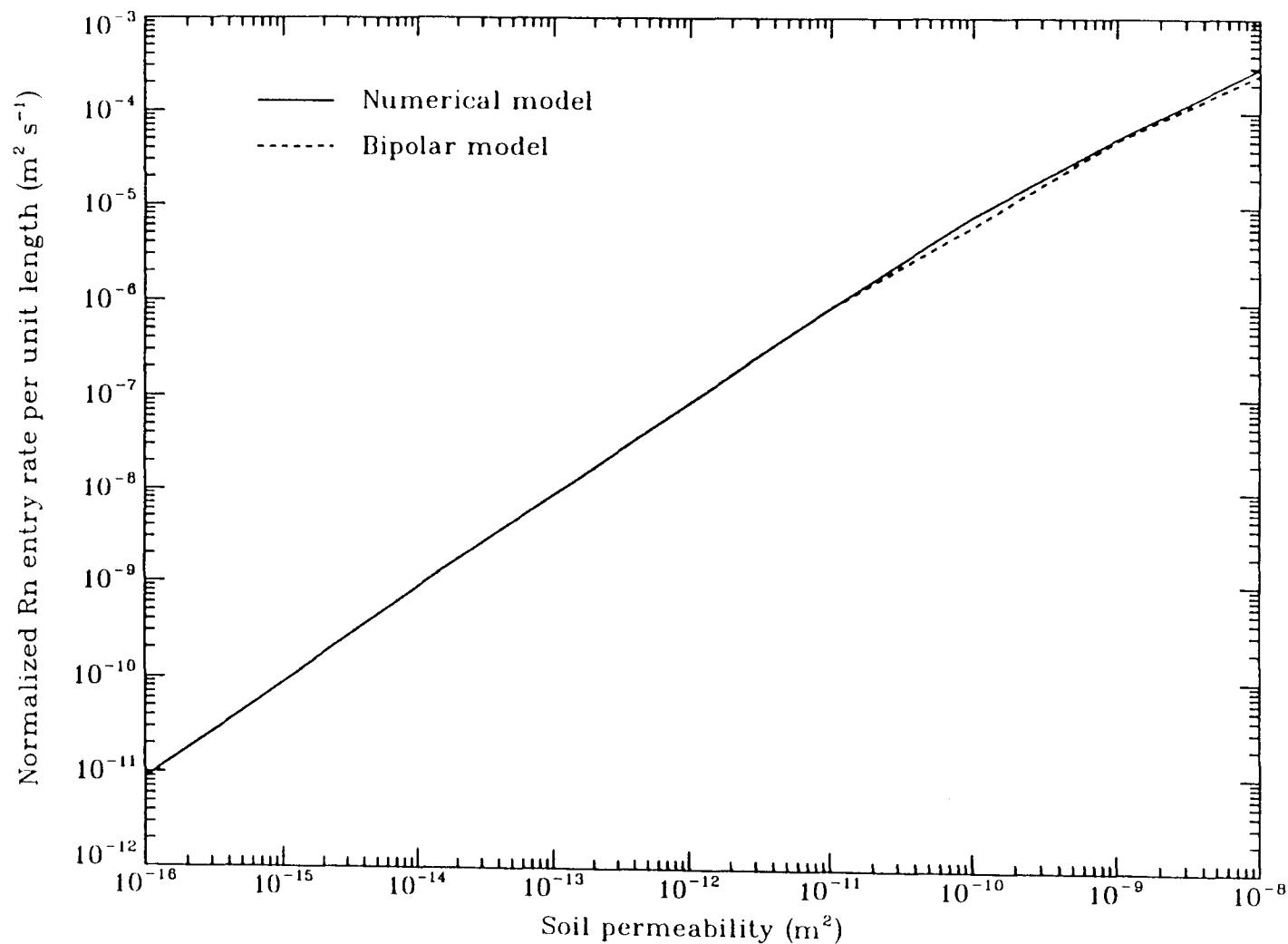
Figure 8.   Comparison of the numerical model without diffusion and the exact solution in bipolar coordinates multiplied by a factor of 0.375. The figure shows the normalized radon entry per unit length of opening for several soil permeabilities, assuming a pressure at the opening of -5 Pa and an opening width of 0.003 m. To obtain results that are independent of soil radium concentration, the entry rates have been normalized by dividing by the radon concentration at a location far from both the house and the soil surface.

43
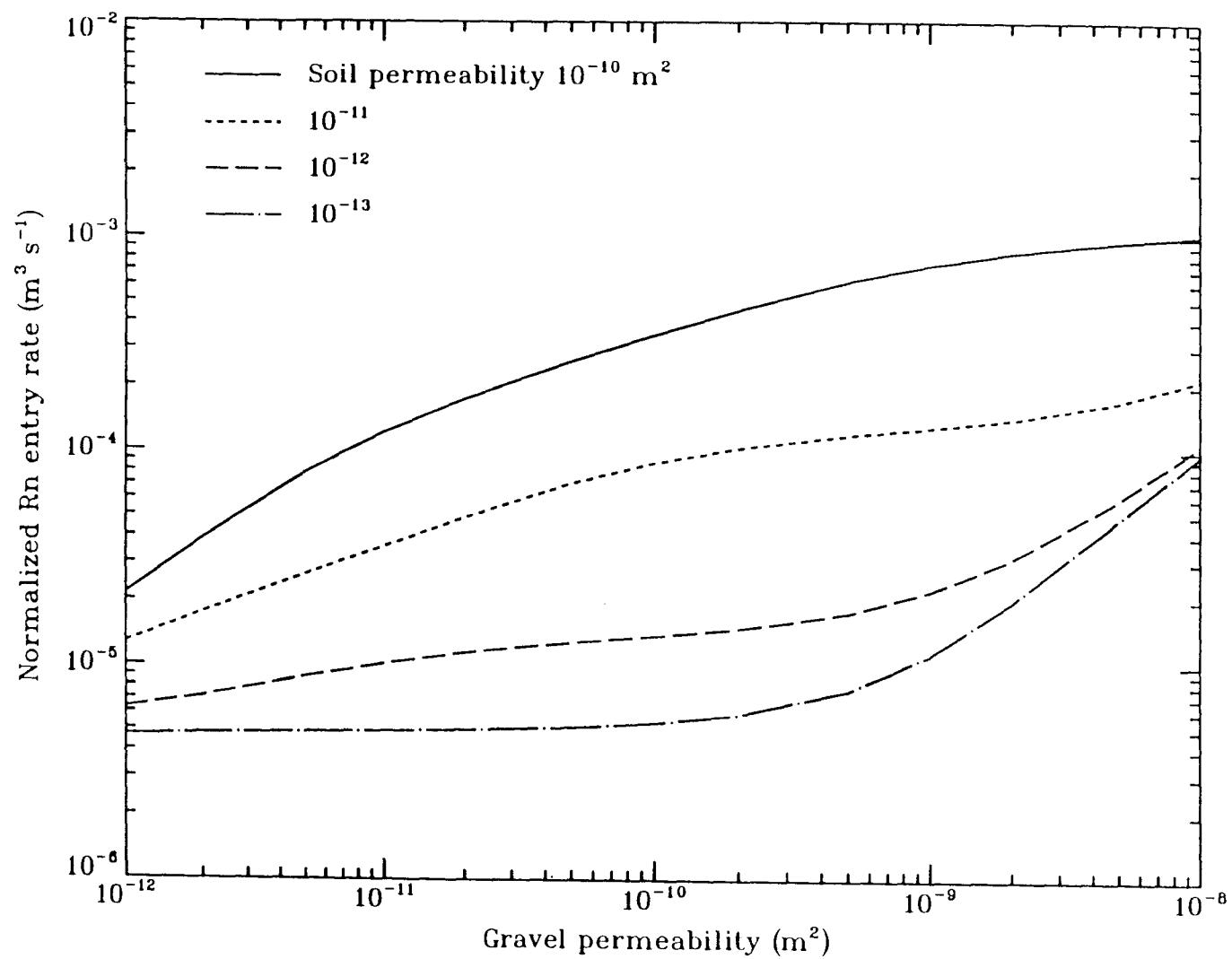
Figure 9. Normalized radon entry rate predictions of the numerical model, assuming a 0.003 m opening at the wall-slab junction, a basement at -5 Pa pressure and a soil block of 10 m radius. The basement depth and radius are 2 m and 5 m, respectively. The soil block is homogeneous except for a gravel bed of thickness 0.15 m beneath the slab.
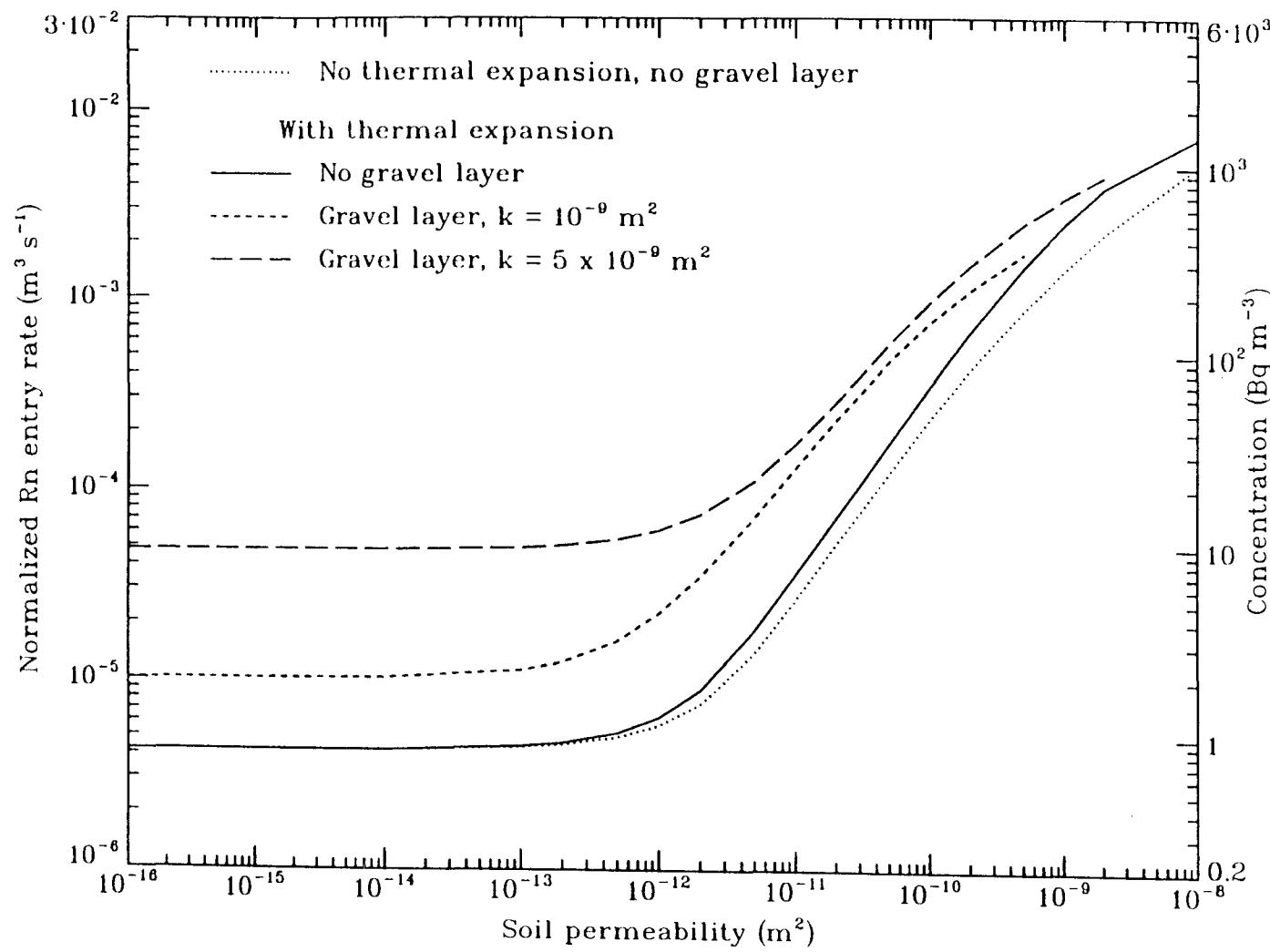
Figure 10. Normalized radon entry rate predictions of the numerical model, assuming a 0.003 m opening at the wall-slab junction, a basement at -5 Pa pressure and a soil block of 10 m radius, for several soil permeabilities. The basement depth and radius are 2 m and 5 m, respectively. The dotted curve shows the entry rate when thermal expansion (buoyancy effects) is excluded from the model. The dashed curves show the effect of a gravel bed under the slab. The right-hand axis shows the radon concentration corresponding to the entry rate for a house of volume 500 m³ and air exchange rate 0.38 h⁻¹ and a soil of radon concentration 10,600 Bq m⁻³.

MODELING TRANSIENT AIRFLOW THROUGH SOILS TOWARDS BUILDINGS

Motivation

Measurements to date (e.g., Nazaroff et al. 1985, 1987; Nazaroff and Nero 1988) indicate that high concentrations of indoor radon are usually due to an elevated rate of radon entry from soil associated with the bulk flow of soil gas. Current reasoning is that the bulk soil gas entry into buildings is driven by small, slowly changing pressure differences (of the order of a few Pa) between the atmosphere and the indoors. This pressure differential may arise due to indoor heating (stack effect), wind, and operation of exhaust fans. If the basement walls are constructed of poured concrete, rather than permeable concrete blocks, the air access from the soil mass to the building is generally restricted to small openings between the basement and the soil (in contrast to permeable substructure surfaces).

The continual pressure difference of a few Pa between a basement and the surrounding soil is considered to be a crucial factor for radon entry. Yet it is well known that barometric pressure fluctuations consist of periodic components with amplitudes ranging from a few Pa for periods of minutes, to a few hundred of Pa, for periods of about a day. Since these amplitudes of pressure variation are comparable to or larger than the pressure differences which apparently drive the steady state flow of soil gas into the house, there exists a definite need to understand how the time-dependent barometric pressure variations influence the soil-gas flux, and ultimately the radon flux, from the soil environment into the building. In our study of transient soil-gas flow we would like to answer the following questions: (1) How does the soil gas flow into a building fluctuate in response to barometric pressure fluctuations and temperature changes? (2) What are the implications of transient soil-gas flux for advective and diffusive radon transport? (3) Is there a region adjacent to the building of particular importance to radon entry? (4) How is the flux variation modified by soil heterogeneity?

Approach

Because of the heterogeneities in the soil, and the complex geometry of the soil structure interface, an advantageous approach for preliminary analysis is to use a numerical model. Researchers in the Earth Sciences Division at LBL have developed codes of various degrees of sophistication to solve problems of isothermal and non-isothermal, single-phase and multiphase fluid flow, as well as transport of dissolved species in variably saturated deformable media. At the present stage of this project, the questions that require immediate resolution concern the understanding of transient, pressure-driven soil-gas flow where the soil gas is primarily air. For this purpose, the isothermal fluid flow model TRUST (Narasimhan et al., 1978) is appropriate. TRUST is based on an Integral Finite Difference Method (IFDM: Narasimhan and Witherspoon, 1976) in which the fluid-mass conservation is implemented over finite elemental volumes of arbitrary shape and gradients of potential are evaluated using finite differences. The model can, in general, handle heterogeneous or anisotropic media, nonlinear boundary conditions and source terms. The code was developed to solve problems of transient flow of a slightly compressible fluid in isothermal, variably saturated, deformable media.

Verification of numerical code

In regard to the flow of water in soils, the code TRUST has been extensively verified against analytical solutions and validated against experimental results for water flow in complicated systems (Narasimhan and Witherspoon, 1978). In principle, TRUST can handle transient gas flow in a porous medium in so far as gas can be idealized as a fluid with constant compressibility. The initial task of the present study is to verify and illustrate the ability of TRUST to handle the transient flow of a gas in a porous medium. The TRUST verification exercise involved two problems for which analytical solutions are available.

The first problem is the radial flow of air to an air sampler from which air is extracted at a constant flowrate. The space-time variation of the pressure head in the "air aquifer" is verified

against the exponential integral solution (widely known as the Theis' solution) found in standard textbooks on groundwater hydrology. The results from numerical simulation compared favorably with the analytic solution, including consideration of "well-bore storage" effects.

The second problem for verification involved the transient propagation of barometric fluctuations through a vertical soil column. The top of the homogeneous column is exposed to the atmosphere, and the bottom is connected to the water table, which is treated either as a no-flux boundary or a boundary with constant potential. Analytical solutions of the amplitude attenuation and phase lag of the barometric pressure for both boundary conditions are available in Carlslaw and Jaeger (1986, p. 105). The simulated results from TRUST showed excellent agreement with the analytic solution for a range of porosity values for the soil column, for air permeability values ranging over 6 orders of magnitude, for barometric periods of 1., 6., and 12 hours, and for discretization of the column ranging from 5 to 100 mesh elements.

For the verification exercise, we have chosen problems with simple geometry and homogeneous material properties for which analytical solutions exist. However, apart from the lack of complexity in geometry and material properties, these examples do encompass processes of transient pressure-driven flow of air through soil which are of relevance to the problem of transport of radon in soil gas.

Analysis Completed

Numerical modeling exercises are intended to help the Small Structure Project in many different ways. These are:

1. to understand and evaluate the relative importance of various physical processes;
2. to aid in the design and choice of instruments and probes;
3. to help in the design of field experiments;
4. to interpret the field experiments; and
5. to predict system response to various remediation strategies.

So far we have addressed the first two aspects, namely, physical process elucidations and the design of probes (probe A described previously).

Instrumentation Design - Response of a Soil Probe

To provide assistance for instrument design, we modeled transient air flow into a cylindrical soil gas sampler, as described in the previous section on instrumentation, considering such factors as the response time of the sampler as a function of sampler dimensions, skin resistance at the sampler probe screen, material properties such as soil porosity, air permeability, air compressibility and effects of a water-saturated land surface. The calculations were carried out in realistic geometries for vertical and horizontal configurations of the probe in the soil formation which was modeled in both two- and three-dimensions. The results obtained aided in the design and choice of probes for measuring permeability.

Transient Air Flow to and around a Basement Under "Barometric Pumping" Boundary Conditions

In the context of the knowledge so far gained about radon entry into houses and the commencement of controlled field experiments at the Ben Lomond site, a very important modeling task is to generate information on the expected patterns of transient air flow between the soil mass and the small structure. Our most recent modeling efforts have been focused in this direction, leading to some useful insights. The salient features of these analyses will be summarized and submitted for publication in the forthcoming special issue of Geophysical Research Letters devoted to radon. In these analyses, the effect of the barometric fluctuations on the transient air (soil-gas) flow into the basement induced by the persistent under pressure at the basement is investigated. The problem is defined as shown schematically in Figure 11. The water table at which a mean air pressure of $\bar{P}_{wt} = 10^5$ Pa is assumed, lies at 5 m below the land surface and 3 m below the basement floor which is given a linear dimension of 10 m. In the initial analyses reported here, the basement has an uncovered soil floor. The soil air within the formation will be static if the gas pressure at each elevation, z, is $P_0(z) = \bar{P}_{wt} - \rho g z$ where ρ is the density of the soil air and g is the gravitational acceleration. The pressure boundary conditions at the land surface and the basement floor which would induce air flow were chosen as follows: The fluctuations in the atmospheric pressure were assumed to be felt at both the land surface and at the basement floor with no damping or phase lag. For our initial studies, the atmospheric pressure fluctuations were assumed to consist of only

one sinusoidal component with a given amplitude and frequency. In addition to the atmospheric fluctuation boundary conditions, the pressure at the basement floor is assumed to be always 5 Pa below that at the land surface. Hence, the periodic pressure was required to oscillate around the mean values, $\overline{P} = P_o$(at z=5m) at the land surface and $\overline{P} = P_o$(at z=3m)-5 Pa at the basement floor.

Simulations of transient air flow were carried out with the above imposed boundary conditions for an appropriate range of soil permeability to air: 0.153, 1.53, and 15.3 × 10^{-12}m^2. Preliminary investigations of the dependence of air flow on the barometric frequency was carried out with two sets of barometric parameters: sinusoidal amplitude of 50 Pa with a period of 30 minutes and an amplitude of 250 Pa with a period of 24 hour.

Results - Transient Air Flow Into a Basement with a Soil Floor

In the absence of the time-dependent sinusoidal variation of the atmospheric pressure, the constant under-pressure of 5 Pa at the basement will induce an air flux into the basement. The magnitude of this steady state air flow entering the half-length (5m) of the basement varied with soil per-meability as tabulated in the second column of Table 6. As to be expected in the case of a linear problem, the steady flux varied linearly with the permeability. In response to the sinusoidal variation of atmospheric pressure, the air flow at the basement also oscillates with the same period, about the values given in column 2 of Table 6. In columns 3 and 4 of Table 6, we list the amplitudes of the flow oscillation for the respective permeabilities and the two different frequencies of barometric pressure variation. Note that except for the last entry in column 4, these amplitudes are much larger than the magnitude of the steady state inflow into the basement in the absence of "barometric pumping". In particular, the magnitude of these fluxes were enhanced by almost two orders of magnitude in column 3 for the lowest permeability case. The net result is that the dynamic system is characterized by *flux reversals*: air moves from the soil into the basement as atmospheric pressure decreases, and moves from the basement into the soil as pressure increases.

To investigate further the reversal of flow directions within the soil medium, we also computed air fluxes (kg/s-m^2) across the vertical plane x = 5 m at the basement edge at four depths: 0.05 m, 0.3 m, 1.0 m and 1.8 m below the basement floor. These are shown in Figure 12. Figure 12a pertains to the low permeability case of 0.153 × 10^{-12}m^2, and Figure 12b pertains to

the high permeability case of 15.3×10^{-12} m^2. Positive values of flux imply flow in the negative x direction, toward the basement. Presence of negative fluxes in Figure 12a show that in fact fluxes periodically move away from the basement. The increase in phase lag with depth of the fluxes, in response to the oscillatory atmospheric pressure, arises from the longer flow paths and increased resistance (from the finite air permeability) with depth. As a result of the finite response time of the medium to the pressure driving force, the fluxes reach "oscillatory equilibrium" (values of extrema remain invariant with cycles) only beyond the third cycle. Results for the high permeability case in Figure 12b show that both the phase lag and the response time to reach "oscillatory equilibrium" are negligible. Furthermore, though the fluxes across the plane x = 5 m oscillate in magnitude, they all have positive sign, indicating that the fluxes across this plane are directed toward the house at all times.

Column 4 of Table 6 shows that for the barometric pressure oscillation with an amplitude of 250 Pa and a period of 24 hours, the amplitudes of the oscillatory fluxes at the basement exceed the steady state fluxes in column 2 for the two smaller permeabilities. However, for the largest permeability case, the amplitude of the oscillatory flux is smaller than the steady state value. These numbers indicate that the fluxes are still alternatively flowing in and out of the basement for the two lower permeability values, but for the largest permeability value, fluxes are always directed into the basement. As to the flow directions within the soil medium, similar plots such as Figure 12 for this low frequency driving pressure case show that the flow direction is exclusively toward the house across the plane x = 5 m.
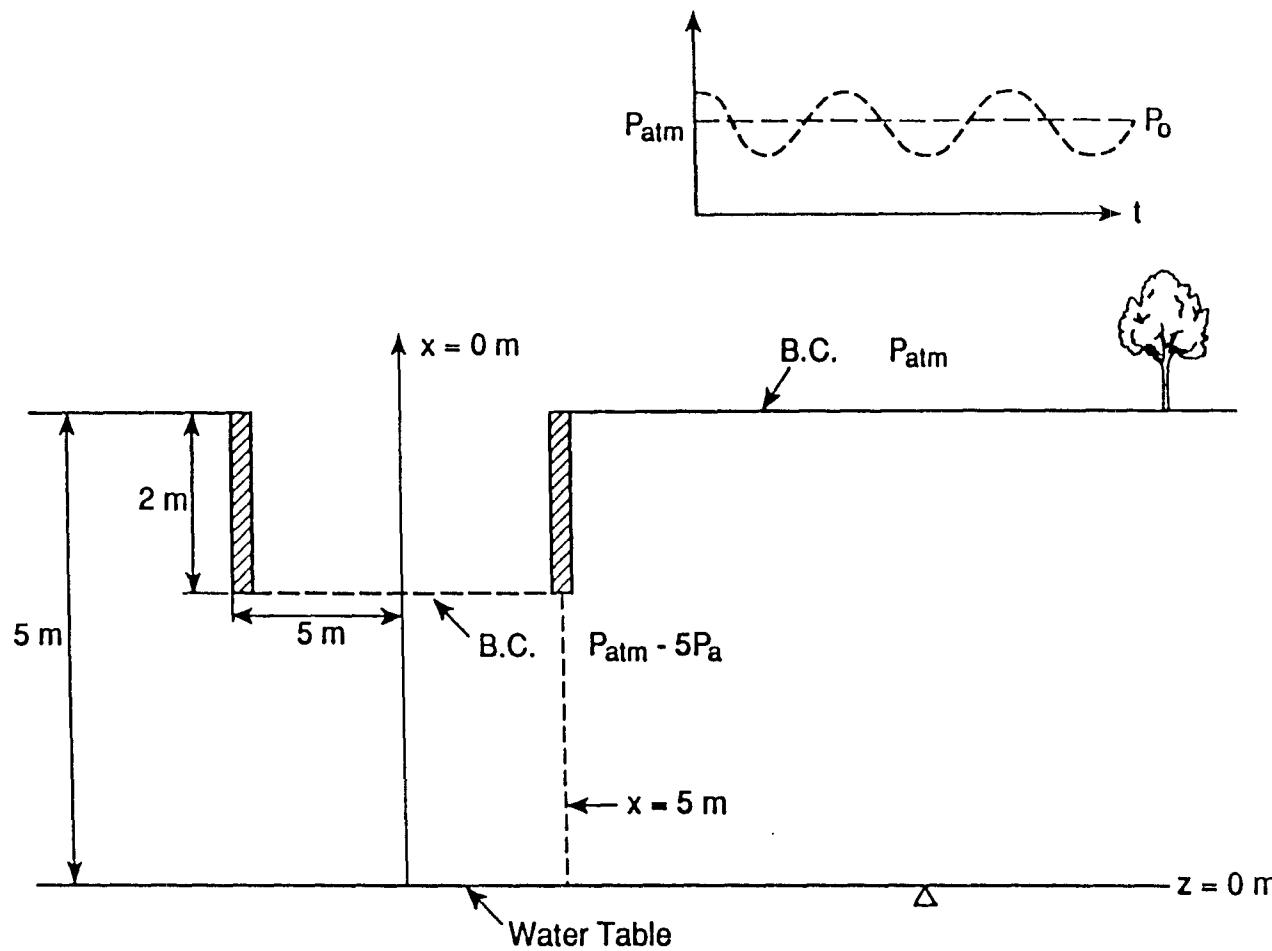
The above results show that effects of barometric fluctuation are strongest in the cases where permeability is low and the fluctuation frequency is high. In these cases, the barometric fluctuation can greatly enhance the magnitude of fluxes as well as introduce flow direction reversals from surrounding soil into the basement. This result is significant because, in the absence of barometric pressure fluctuations, convective (bulk) flow plays an important role in accounting for high radon entry rate into basements only in soil with a high permeability to air. Our calculations have identified a flow process by which air flow through a low permeability medium may also be large due to the larger time-dependent driving force. Since a real soil system, even of intrinsically high permeability, is characterized by heterogeneities arising from both material property distributions as well as from variations with water saturation, these transient processes that are dominant

in low permeability media may significantly impact the transport of radon from soil to house even at sites with a high spatial-average permeability. In addition, we have just addressed a single component in the barometric fluctuation, whereas the real barometric variation will comprise many periods which may not necessary be in phase. The effects of these realistic parameter variations are presently being studied to provide valuable information on the air flow-radon advection relationships.

The next major directions of this transient modeling will be to model soil-gas flow into a more typical basement with a concrete floor, discrete openings to the soil, and with and without a layer of aggregate beneath the floor. In addition, radon generation, transport, and decay will be added to the transient model. Firm conclusions regarding the importance of transient flow to radon entry must await this future modeling and the collection of data from transient experiments.

Table 6.   Air flow at basement floor with constant under pressure of 5 Pa in the absence and presence of barometric pumping

Permeability K(10^{-12} m^2)	Air Flow (10^{-6} kg/s)		
	Steady State flow with no barometric pumping	Amplitude of Oscillatory flow with barometric pumping	
		A = 50Pa T = 0.5 hr	A = 250Pa T = 24 hr
0.153	0.041	2.85	1.17
1.53	0.41	10.1	1.18
15.3	4.1	16.3	1.20

Figure 11. Problem definition for modeling air (soil-gas) flow in the presence of barometric fluctuations and a constant underpressure of 5 Pa at the basement.
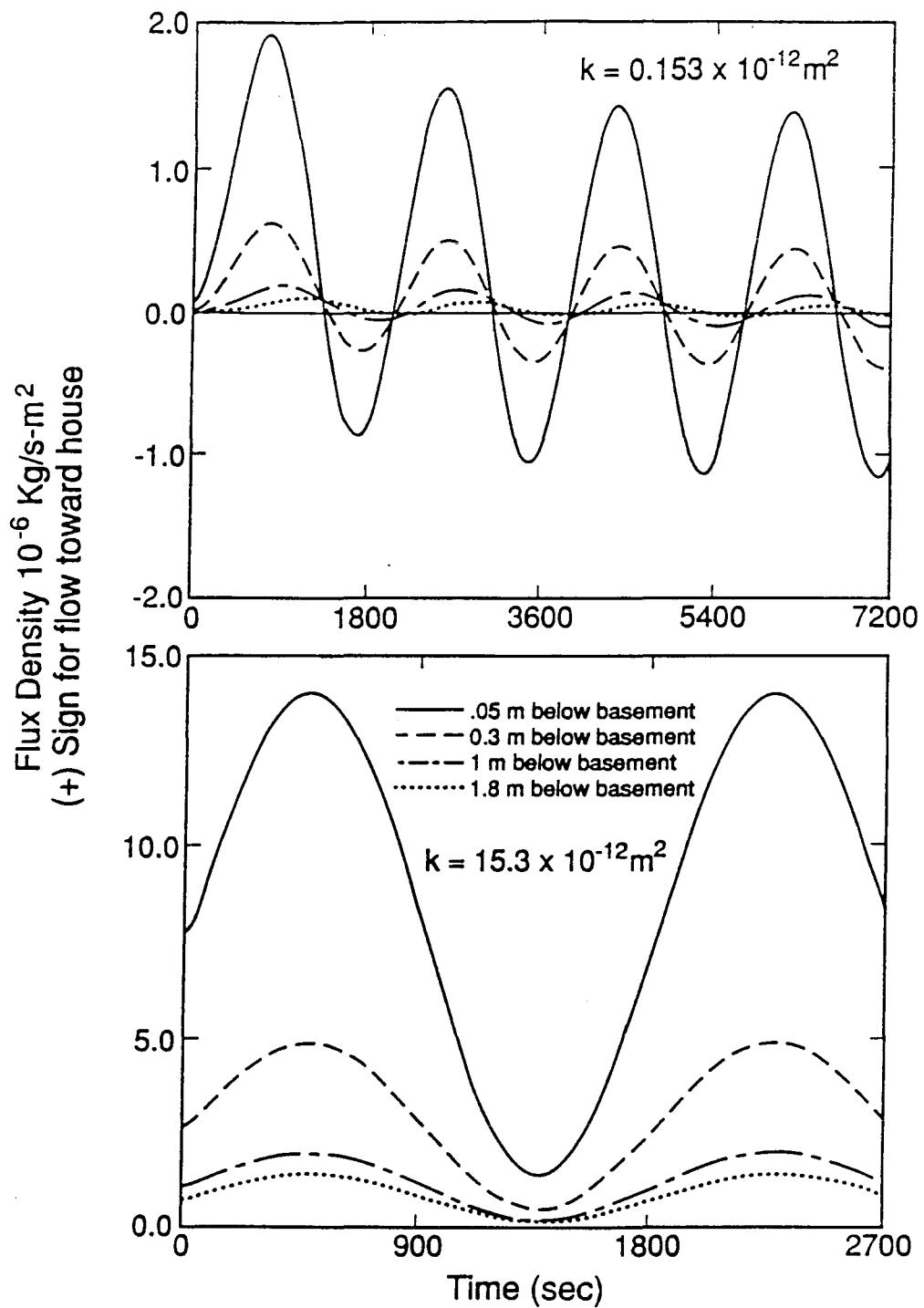
Figure 12. Air flow across vertical plane x = 5 m at basement edge for constant under pressure of 5 Pa and barometric pumping of amplitude 50 Pa and period 0.5 hr.

XBL 898-7701
T.I.D. Illus.88

SUMMARY OF MAJOR ACCOMPLISHMENTS

Two unique, room-size basements, ideally suited for experimental research on radon entry, have been designed and constructed at a field site and characterization of the soils surrounding the structures is underway. A state-of-the-art instrumentation system has been designed and is being installed. In the course of developing instrumentation for use with these structures, we have designed and fabricated a new type of probe for measuring, with substantially increased accuracy, the air permeability of soil. Procedures for accurate multipoint measurement of radon concentrations using a continuous radon monitor have been improved and verified. Steady-state numerical modeling has indicated that buoyancy-driven flow and layers of subslab aggregate can, under some conditions, cause large increases in the rate of radon entry into buildings. Transient numerical modeling has indicated that transient soil-gas flow, driven by atmospheric pressure variations, may be an important process of radon entry into structures surrounded by relatively low-permeability soils.

REFERENCES

Bowman, R. H. and D. C. Estrada (1980) "Soil survey of Santa Cruz County, California"; U.S. Department of Agriculture, Soil Conservation Service.

Busigin, A., A.W. Van Der Vooren, and C.R. Phillips (1979). "Interpretation of the response of continuous radon monitors to transient radon concentrations," *Health Physics,* 37 pp. 659-667.

Carlslaw, H. S., and J. C. Jaeger (1986). *Conduction of Heat in Solids, 2nd Ed.,* Oxford Science Publications, Oxford, England, 510 pp.

DSMA Staff (1983). "Review of existing instrumentation and evaluation of possibilities for research and development of instrumentation to determine future levels of radon at a proposed building sites." DSMA Acton Ltd. Report INFO-0096.

DSMA Staff (1985). "A computer study of soil-gas movement into buildings." DSMA Acton Ltd. Report No. 1389/1333.

Edwards, A.L. (1969). "TRUMP: A computer program for transient and steady-state temperature distribution in multi-dimensional systems," NTIS, UCRL 14754, Rev. II, Springfield, VA 22151.

Garbesi, K (1988). "Experiments and Modeling of the Soil Gas Transport of Volatile Organic Compounds into a Residential Basement." M.S. Thesis, Lawrence Berkeley Laboratory Report, LBL-25519 Rev.

Garbesi, K. and R.G. Sextro (1989). "Modeling and Field Evidence of Pressure-Driven Entry of Soil Gas into a House Through Permeable Below-Grade Walls." Accepted for publication in *Environmental Science and Technology.*

Lambert, G., and J. Kashiwagi (1978). "Soil Survey of Napa County, California"; U.S. Department of Agriculture, Soil Conservation Service.

Leo, G. (1967). "The plutonic and metamorphic rocks of the Ben Lomond Mountain area, Santa Cruz County, California": Calif. Div. Mines and Geology Special Report 91, p. 27 - 43.

Loureiro, C.O. (1987) "Simulation of the steady-state transport of radon from soil into houses with basements under constant negative pressure." Ph.D. Thesis. Lawrence Berkeley Laboratory Report, LBL-24378.

Mowris, R.J. and Fisk, W.J. (1988) "Modelling the effects of exhaust ventilation on radon entry rates and indoor radon concentrations." *Health Physics* (54), pp. 491-501.

Narasimhan, T.N. (1975). "A unified numerical model for saturated-unsaturated ground water flow," Ph.D. Thesis, Lawrence Berkeley Laboratory Report, LBL-8862.

Narasimhan, T. N., and P. A. Witherspoon (1976). "An integrated finite difference method for analyzing fluid flow in porous media." *Water Resources Research,* 12(1), pp. 57-64.

Narasimhan, T. N., and P. A. Witherspoon (1977). "Numerical model for saturated-unsaturated flow in deformable porous media 1. theory," *Water Resources Research,* 13(3), pp. 657-664.

Narasimhan, T. N., A. L. Edwards, and P. A. Witherspoon (1978). "Numerical model for saturated-unsaturated flow in deformable porous media 2. The Algorithm," *Water Resources Research,* 14(2), pp. 255-261.

Narasimhan, T. N., and P. A. Witherspooon (1978). "Numerical model for saturated-unsaturated flow in deformable porous media, Part III: Applications," *Water Resources Research,* 14(6), pp. 1017-1034.

Nazaroff, W. W., H. Feustel, A. L. Nero, K. L. Revzan, and D. T. Grimsrud (1985). "Radon transport into a detached one-story house with a basement," *Atmospheric Environment* 19(1), pp. 31-46.

Nazaroff, W.W. (1988) "Predicting the rate of ^{222}Rn entry from soil into the basement of a dwelling due to pressure-driven air flow." *Radiation Protection Dosimetry* 24 (1/4), pp. 199-202.

Nazaroff, W. W., S. R. Lewis, S. M. Doyle, B. A. Moed, and A. V. Nero (1987). "Experiments on pollutant transport from soil into residential basements by pressure-driven airflow," *Environmental Science & Technology,* 21, pp. 459-466.

Nazaroff, W.W. and Sextro, R.G., (1989) "Technique for measuring the indoor ^{222}Rn source potential of soil." *Environmental Science and Technology,* 23, 4, p. 451

Nazaroff, W. W., B. A. Moed, R. G. Sextro, K. L. Revzan, and A. V. Nero (1989a). "Factors influencing soil as a source of indoor radon: a framework for geographically assessing radon source potentials," Lawrence Berkeley Laboratory Rept. LBL-20645.

Nazaroff, W.W. and Nero, A.V., editors (1988). *Radon and Its Decay Products in Indoor Air.* J. Wiley & Sons, New York. ISBN 0-417-62810-7.

Patankar, S.V. (1980). *Numerical Heat Transfer and Fluid Flow.* Hemisphere, New York, NY.

Revzan, K.L. (1989). "Radon entry, distribution, and removal in two New Jersey houses with basements." Lawrence Berkeley Laboratory Report, LBL-26830. To be published in *Health Physics.*

Revzan, K.L., Fisk, W.J., and Gadgil, A.J. (1989). "The influence of soil permeability on radon entry into houses with basements." In draft.

Turk, B.H., Prill, R.J., Grimsrud, D.T., Moed, B.A., and Sextro, R.G. (1989). "Characterizing the occurrence and variability of radon in Pacific Northwest homes." Lawrence Berkeley Laboratory Report, LBL-26960. Submitted to *JAPCA.*

Turk, B.H., Prill, R.J., Sextro, R.G., and Harrison, J. (1988). "Intensive radon mitigation research: lessons learned." Proceedings of the 81st Annual Meeting of the Air Pollution Control Association, June 19-24, Dallas. Lawrence Berkeley Laboratory Report, LBL-25910.

Weeks, E. P. (1978). "Field determination of vertical permeability to air in the unsaturated zone," U.S. Geological Survey Professional Paper 1051, U. S. Government printing office, Washington, 41 pp.

Welch, L. E., R. C. Huff, R. A. Dierking, T. D. Cook, L. A. Bates, and W. F. Andrews (1966). "Soil survey of the Alameda area, California"; U.S. Dept. of Agriculture, Soil Conservation Service.

Wollenberg, H. A. and K. L. Revzan (1989). "Radium regionalization in California," submitted to *Geophysical Research Letters*.